

**The Determination of  $^{210}\text{Pb}$  by Accelerator Mass Spectrometry**

Adam Sookdeo B.Sc (Hons)

Thesis submitted to the  
Faculty of Graduate and Postdoctoral Studies  
in partial fulfillment of the requirements for the  
Specialization MSc degree in Environmental and Chemical Toxicology (Earth Sciences)

Ottawa-Carleton Geoscience Centre  
Department of Earth Sciences  
Faculty of Science  
University of Ottawa

September 2014

© Adam Sookdeo, Ottawa, Canada, 2015

## Abstract

The aim of this thesis was to establish a methodology for  $^{210}\text{Pb}$  measurements by Accelerator Mass Spectrometry (AMS). The potential application is to measure  $^{210}\text{Pb}$  in people who have been exposed to radon. This will better our understanding of radon toxicity, which is not possible now with current radiometric and mass spectrometry techniques. The determination of  $^{210}\text{Pb}$  by AMS was done in two major studies 1) Studying Pb chemistry in a  $\text{Cs}^+$  sputter source used in AMS and 2) Evaluating  $^{204,205}$  &  $^{208}\text{Pb}$  spikes for the quantification of  $^{210}\text{Pb}$  by isotope dilution.

Pb chemistry was investigated using an 834 SIMS-type and a SO-110  $\text{Cs}^+$  sputter source at the IsoTrace Laboratory and A.E Lalonde AMS facility, respectively. Different molecular anions of Pb were studied with the 834 SIMS-type  $\text{Cs}^+$  sputter source and the strongest molecular anion current of Pb and thus greatest ionization efficiency was achieved from the superhalogen  $\text{PbF}_3^-$ . The average  $^{208}\text{PbF}_3^-$  current was unaffected by varying the ratio of the fluorinating compounds ( $\text{AgF}_2$  and  $\text{CsF}$ ) packed into a target. The average current of  $^{208}\text{PbF}_3^-$  was reproducibly increased by chemically mixing the targets of  $\text{AgF}_2$ ,  $\text{CsF}$  and  $\text{PbF}_2$  in concentrated HF rather than mechanically mixing them the powders with a stir rod. The count rate of  $^{210}\text{Pb}$  reproducibly increased by a factor of 20 when  $\mu\text{g}$  quantities of  $\text{PbF}_2$  were present in mg AMS targets compared to AMS targets that had pg quantities of  $\text{PbF}_2$ . The average current of  $^{208}\text{PbF}_3^-$  for pure  $\text{PbF}_2$  targets in an SO-100  $\text{Cs}^+$  sputter source was reproducibly increased when the  $\text{Cs}^+$  flux was decreased by a factor of 10. This phase of my work maximized the overall efficiency of  $\text{PbF}_3^-$ , to a value of  $1.8 \times 10^{-10} \pm 8 \times 10^{-11} \text{ s}^{-1}$ , which was a key first step in the measurement by AMS. Then isotope dilution was tested to quantify  $^{210}\text{Pb}$  and the next stage of my work evaluated the use of  $^{204,205}$  &  $^{208}\text{Pb}$  spikes.

$^{210}\text{Pb}$  was measured in the +3 charge state by isotope dilution assays using  $^{204,205}$  &  $^{208}\text{Pb}$  spikes.  $^{204}\text{Pb}^{+3}$  reproducibly suffered from the molecular interference from  $^{68}\text{Zn}_3^{+3}$ , which could not be easily removed without negatively impacting the detection limit for  $^{210}\text{Pb}$ .  $^{205}\text{Pb}^{+3}$  continually suffered from  $^{205}\text{Tl}^{+3}$  interference which could be readily be removed but not without negatively affecting the

detection limit for  $^{210}\text{Pb}$ .  $^{208}\text{Pb}^{+3}$  suffers from no molecular interferences but if a large amount of  $^{208}\text{Pb}$  is needed to swamp the Pb in a sample, this could limit the detection limit for  $^{210}\text{Pb}$  as the abundance sensitivity is  $^{210}\text{Pb}/^{208}\text{Pb}=1.3\times 10^{-12}$ . A calibration curve is required when  $^{208}\text{Pb}$  is used as a spike due to a difference in collection efficiency of a Faraday cup, where  $^{208}\text{Pb}^{+3}$  is detected and the gas ionization chamber, where  $^{210}\text{Pb}^{+3}$  is detected. The quantification of  $^{210}\text{Pb}$  with  $^{208}\text{Pb}$  as a spike yielded a detection limit of 4.4mBq at the IsoTrace facility. A theoretical detection limit of  $\leq 0.11\text{mBq}$  is expected at the A.E Lalonde AMS facility. The expected detection limit at the A.E Lalonde AMS facility is on par with  $\alpha$ -spectroscopy but AMS samples can be counted in less than 1 hour whereas alpha spectrometry samples must be counted for about 1 day.

## Acknowledgments

I would like to thank Dr. Jack Cornett for providing me with the opportunity to pursue this research, and for his critical review of this thesis. His patience, eagerness, positivity, and the immeasurable amount of time he spent on this project as well as his support are greatly appreciated! In addition, I am grateful to his willingness and eagerness see this work presented at both national and international conferences and submitted to scientific journals.

I also gratefully acknowledge those who have helped me along the way, especially Dr. Xiaolei Zhao for operating and constantly explaining the intricacies of Accelerator Mass Spectrometry (AMS). I would also like to thank Dr. Liam Kieser for helping take a physical approach to AMS, Dr. Chris Charles for helping me with column chemistry and quantifying the  $^{205}\text{Pb}$  spike. To Dr. Nimal De Silva I am grateful to you for all the advice and discussion we had about extraction and precipitation chemistry along with all the ICP-MS measurements you did for this project. I would like to acknowledge Dr. Ted Litherland for the invaluable ideas you generated during our coffee breaks and lunches at the library in Isotrace. I would also like to acknowledge the scholarship I received from G.G Hatch Stable Isotope Laboratory and the TD Green Bursaries I received, I am grateful for the financial support you provided me during this project.

I would also like to thank my family. My mother, for her constant support and guidance without her I would have never completed this project, my brothers Matt, Martin and Ryan who always keep me grounded and to Taylor who has probably learnt more about AMS and radioisotopes than she ever wanted.

I wouldn't have gotten through grad school without the great friends I made along the way at uOttawa; Jack Dann, Stacey Wetmore, Micheal James, Erin Adlakha, Mary Devine, Octavia Bath, David Diekrup Shamus Duff, Émilie Gagnon, Kristina Boros and David Lowe. I do not think one of

you escaped my rants about AMS. Lastly, I would like to say am grateful for the opportunity and the experience I gained while completing this project.

## List of Publications

This is a paper-format thesis. It is based on work presented in the following publications:

- I A. Sookdeo<sup>1\*</sup>, J. Cornett<sup>1</sup>, X.-L. Zhao<sup>2</sup>, W. E. Keiser<sup>2</sup>  
Production of Pb beams for <sup>205,210</sup>Pb analysis by AMS  
To be submitted to Nuclear Instruments and Methods in Physics Research B.
- II A. Sookdeo<sup>1\*</sup>, J. Cornett<sup>1</sup>, X.L. Zhao<sup>2</sup>, C.R.J Charles<sup>2</sup>, & W. E. Keiser<sup>2</sup>  
Quantifying <sup>210</sup>Pb by Accelerator Mass Spectroscopy: A study of molecular and isobaric interferences of <sup>204,205,208</sup>Pb and <sup>210</sup>Pb  
To be submitted to Rapid Communications in Mass Spectrometry.

## Contributions

A Selection of Conferences attended:

- Attendee of Pittcon Conference and Expo March 2013. Philadelphia, Pennsylvania, USA.
- Presenter (oral) at 96<sup>th</sup> Canadian Chemistry Conference and Exhibition May 2013.  
Determination of <sup>210</sup>Pb by Accelerator Mass Spectrometry. Quebec city, Quebec, Canada.
- Presenter (oral) at EnviroAnalysis September 2013. Determination of <sup>210</sup>Pb by Accelerator Mass Spectrometry. Toronto, Ontario, Canada.
- Attendee of Prospectors and Developers Association of Canada, March 2014. Toronto, Ontario, Canada.
- Presenter (oral) at The Advances in Earth Sciences Research Conference March 2014. <sup>210</sup>Pb measurements by AMS, a look at <sup>204,205 & 208</sup>Pb spikes. Ottawa, Ontario, Canada
- Presenter (oral) at the Canadian Association of Physicists Congress, June 2014. Production beams of <sup>205</sup>Pb and <sup>210</sup>Pb using a Cs<sup>+</sup> sputter source in an AMS. Sudbury, Ontario, Canada.
- Presenter (oral) at the 13<sup>th</sup> Accelerator Mass Spectrometry conference, August 2014.  
Production of <sup>205,210</sup>Pb beams for analysis by Accelerator Mass Spectrometry. Aix en Provence, Provence, France.

### **International Accelerator Mass Spectrometry visits**

- Radiocarbon Dating Laboratory, Lund University February 2014. Lund, Sweden.
- Tandem Laboratory, Uppsala University, February 2014. Uppsala, Sweden
- Ion Beam Physics, ETH-Zurich, February 2014. Zurich, Switzerland.

### **Statement of Originality**

The work presented in this thesis was written by me with crucial input and critical review by Dr. Robert J. Cornett. The research was done by myself at IsoTrace Laboratory located in Toronto, Canada and the A.E Lalonde facility at the University of Ottawa. The accelerators were operated by Dr. X-L. Zhao. I worked with him to perform the measurements that are reported in this work.

## Table of Contents

Abstract .....	II
Acknowledgments .....	IV
List of Publications.....	VI
Contributions .....	VI
International Accelerator Mass Spectrometry visits .....	VII
Statement of originality .....	VII
List of figures .....	X
List of tables .....	XI
Chapter 1 .....	1
Introduction .....	1
Background .....	4
Thesis outline .....	10
Reference.....	11
Chapter 2 .....	15
Abstract .....	15
Introduction .....	16
Cs <sup>+</sup> sputtering on PbF <sub>2</sub> targets.....	17
Molecular Anions of Pb .....	18
Chemical compositions of PbF <sub>2</sub> targets affect on <sup>208</sup> PbF <sub>3</sub> <sup>-</sup> current .....	19
Mechanical mixing compared to chemically fluxing PbF <sub>2</sub> targets affect on <sup>208</sup> PbF <sub>3</sub> <sup>-</sup> current....	20
Concentration of µg of common PbF <sub>2</sub> compared to pg of <sup>205</sup> PbF <sub>2</sub> affect on <sup>210</sup> Pb count rate....	21
Cs <sup>+</sup> flux affect on <sup>208</sup> PbF <sub>3</sub> <sup>-</sup> current .....	22
Conclusions .....	23
References .....	24

Chapter 3 .....	32
Abstract .....	32
Introduction .....	33
Experimental .....	34
Results and discussion.....	35
Conclusion.....	43
References .....	44
Chapter 4 .....	46
Conclusion.....	46

## List of Figures

<b>Figure 1:</b> Decay scheme for $^{238}\text{U}$ . Image modified from <a href="http://www.hc-sc.gc.ca/ewh-semt/radiation/radon/decay_scheme-eng.php">http://www.hc-sc.gc.ca/ewh-semt/radiation/radon/decay_scheme-eng.php</a> accessed 2014 .....	1
<b>Figure 2:</b> Decay scheme for $^{210}\text{Pb}$ . Image modified from Lariviere <i>et al.</i> 2006.....	4
<b>Figure 3</b> Schematic of AMS at IsoTrace. Modified from MacDonald 2014.....	6
<b>Figure 4</b> $^{208}\text{PbXY}^-$ currents from different chemical mixtures .....	29
<b>Figure 5</b> $^{210}\text{Pb}$ counts for targets with 1Bq of $^{210}\text{Pb}$ spiked with either 5.4pg of $^{205}\text{Pb}$ or 200 $\mu\text{g}$ of common Pb. All targets were packed with equal parts by weight of CsF and $\text{AgF}_2$ . The number of counts recorded in each experiment is shown above the bar .....	30
<b>Figure 6</b> $^{208}\text{PbF}_3^-$ current generated at different $\text{Cs}^+$ fluxes from pure $\text{PbF}_2$ targets .....	31
<b>Figure 7</b> An SEM image of a Pb target after $\text{Cs}^+$ sputtering. The highlighted 1 indicates the single spot method while the un-highlighted numbers indicated a 16 spot method .....	37
<b>Figure 8</b> Current measurements of $^{204}\text{Pb}^{+3}$ for targets spiked with 250 $\mu\text{g}$ of $^{204}\text{Pb}$ . The $\text{Cs}^+$ sputter source was changed from a single spot method to 16 spot method at 475 seconds.....	38
<b>Figure 9</b> Counts at mass-to-charge 205 for blanks of $\text{AgF}_2$ and blanks of $\text{AgF}_2$ and CsF. Note the log scale. ....	39
<b>Figure 10</b> Counts of $^{70}\text{Zn}^{+1}$ and $^{140}\text{Ce}^{+2}$ at mass-to-charge $^{210}/_3$ pre- and post treatment with $\text{Ag}1\times 8$ column. Targets were composed of CLV-1 packed with $\text{AgF}_2$ and CsF and each target was counted for 360 seconds .....	40
<b>Figure 11</b> Calibration curve for $^{210}\text{Pb}$ counts with respect to $^{208}\text{Pb}$ spike count timed ranged 1280-3000s .....	42

## List of Tables

<b>Table 1</b> Measurement techniques for $^{210}\text{Pb}$ .....	2
<b>Table 2</b> Ratios and measurements of $\text{PbXY}^-$ compounds mixed with fluorinating agents or Ag. Currents of $\text{PbXY}^-$ on a 834 SIMS type ion source at IsoTrace.....	25
<b>Table 3</b> Current of $^{208}\text{PbF}_3^-$ generated from targets composed with different ratios by weight of $\text{PbF}_2$ : $\text{AgF}_2$ and $\text{CsF}$ .....	26
<b>Table 4</b> $^{208}\text{PbF}_3^-$ currents from targets composed of 0.2mg of Pb and equal parts of $\text{AgF}_2$ and $\text{CsF}$ . Currents of $\text{PbF}_3^-$ were collected after ESA-1 and measured 10mins after an initial 5min of $\text{Cs}^+$ sputter.....	27
<b>Table 5</b> Mass-to-charge interferences for Pb isotopes.....	36
<b>Table 6</b> Measurements of targets spiked with known amounts of $^{208}\text{Pb}$ and known activity of $^{210}\text{Pb}$ . All targets were packed with equal parts by weight of $\text{AgF}_2$ and $\text{CsF}$ .....	41
<b>Table 7</b> Detection limits for $^{210}\text{Pb}$ at the IsoTrace Laboratory and A.E Lalonde Laboratory.....	43

## CHAPTER 1

### Introduction

$^{210}\text{Pb}$  is a naturally occurring radioisotope with a half-life of 22.3 years and belongs to the  $^{238}\text{U}$  decay series, figure 1.  $^{210}\text{Pb}$  is the longest lived radioisotope in the series after the decay of  $^{222}\text{Rn}$  (Oldfield & Appleby 1984). Since  $^{222}\text{Rn}$  (hereafter Rn) is a noble gas, Rn and all of its decay products including  $^{210}\text{Pb}$  often are not in secular equilibrium with  $^{226}\text{Ra}$  and other longer lived members of the uranium series decay chain. As a result  $^{210}\text{Pb}$  has been used in fields of geochronology and environmental radioactivity or radiation exposure (Rubin *et al.* 2005; Ladinskaya *et al.* 1973).

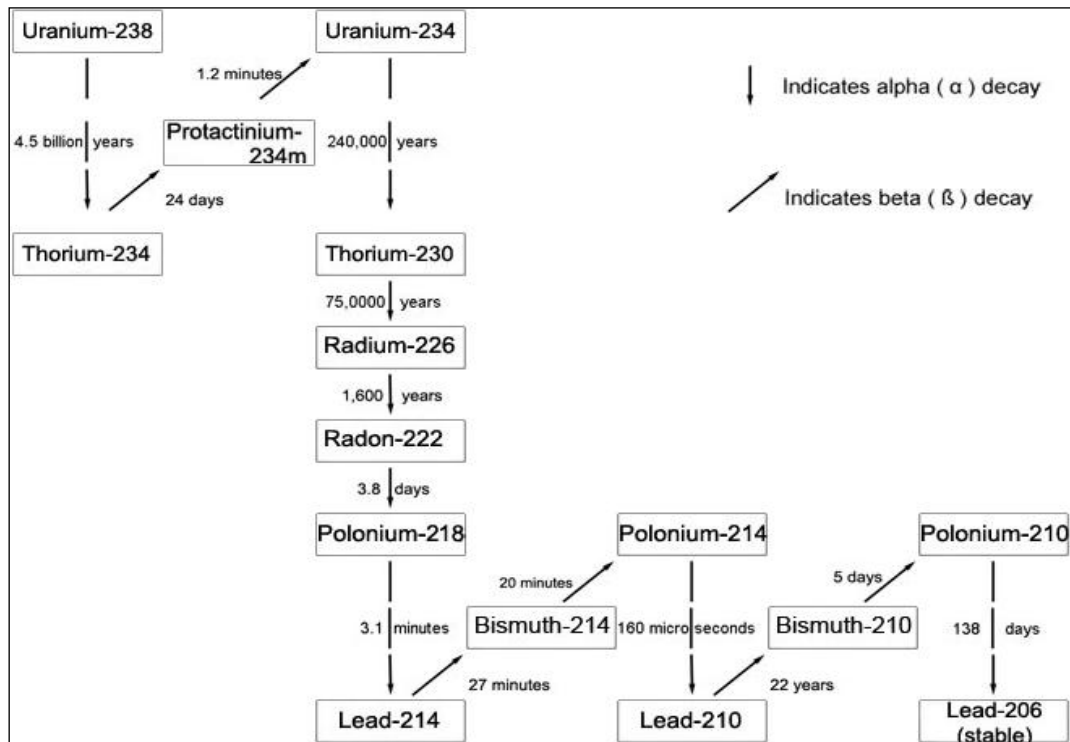


**Figure 1** Decay scheme for  $^{238}\text{U}$ . Image modified from [http://www.hc-sc.gc.ca/ewh-semt/radiation/radon/decay\\_scheme-eng.php](http://www.hc-sc.gc.ca/ewh-semt/radiation/radon/decay_scheme-eng.php) accessed 2014

Inhalation of radon and subsequent exposure in the lung to the short lived radioactive decay products of radon is the second leading cause of lung cancer in Canada (Stewart & Kleihues 2003). In Europe, radon accounts for 2% of all lung cancer deaths for cigarette smokers and ex-cigarettes

smokers (Darby *et al.* 2005). That is why radon activity is measured in homes and offices around the world. To determine radon levels in people it must be done indirectly via  $^{210}\text{Pb}$  as radon has a short half-life (3.8days) as do its progeny (Richardson *et al.* 1991; Wahl *et al.* 2000). Measurements to date of  $^{210}\text{Pb}$  in people involved individuals with high exposure to radon (Eisenbud 1969; Beir 1999). The lack of  $^{210}\text{Pb}$  measurements in individuals exposed to lower, more average levels of radon, is due to the poor detection limits of radiometric and mass spectrometry techniques for  $^{210}\text{Pb}$  in people, table 1 (Al-Zoughool *et al.* 2009). Age, gender, weight, height and other variables affect radon inhalation and subsequent exposure and the risk of lung cancer. The variable individual response along with the lack of direct  $^{210}\text{Pb}$  measurements in people has forced regulatory groups to focus upon the level of Rn in air which is not directly correlated with the radiation risk to the individual. This disconnect has led to levels of regulation and concern for indoor radon that vary from country to country.

**Table 1** Measurement techniques for  $^{210}\text{Pb}$ .

<b>Technique</b>	<b>Detection limit</b>	<b>Measurement time +sample preparation</b>
Inductively Coupled Plasma-Mass Spectroscopy (ICP-MS)	90 mBq/L	Minutes + 2 days
Collision Cell ICP-MS	698 mBq/L	Minutes + 2days
$\gamma$ -spectrometry	440 mBq	1000min (no sample preparation required)
Liquid scintillation counter ( $\beta$ -spectrometry)	7 mBq	8-9days +in-growth period
$\alpha$ -spectrometry	0.1-1mBq	3-5days + 3-5month in-growth period

The levels of concern for indoor radon vary from 100-400Bq/m<sup>3</sup> throughout the world, while the World Health Organization (2009) called for tighter standards on indoor radon, stating that

levels of indoor radon should not exceed 300mBq/m<sup>3</sup> (Zielinski *et al.* 2006). However, in Japan, radon therapy in the form of inhalation, bath, or steam is used to treat rheumatic diseases (Falkenbach 2001; Erickson 2005). This discrepancy warrants better understanding of radon toxicity, which may be possible if <sup>210</sup>Pb measurements post-exposure to radon were possible. Accelerator Mass Spectrometry (AMS), a technique renowned for its low detection limits, may provide a new way to measure <sup>210</sup>Pb in people.

The scope of this thesis is to develop a method to determine <sup>210</sup>Pb by AMS and to test the hypothesis that AMS can achieve better detection limits than the aforementioned radiometric and mass spectrometric detection limits.

The method development was done in multiple steps. First, a variety of molecular anions of Pb were investigated in a sputter source to determine the molecular anion that had the greatest ionization efficiency and thus provided the highest beam current and hopefully the lowest detection limit. Second, the chemistry of the molecular anions was then further explored to determine if the ratio of chemicals in a Pb target influenced the ionization efficiency. To test for further increases in the ionization efficiency, the homogeneity of the target prepared by fluxing in acid compared to mechanical mixing was also investigated. Third, to quantify <sup>210</sup>Pb by AMS using isotope dilution, the addition of known amount of an isotope to the sample to be analyzed in order to quantify the isotope of interest (Ostrowski 1968). Isotopes investigated as possible spikes for isotope dilution of <sup>210</sup>Pb were <sup>204</sup>Pb, <sup>208</sup>Pb and <sup>205</sup>Pb. <sup>204</sup>Pb and <sup>208</sup>Pb were spiked in µg quantities to swamp natural levels in samples and measured in a Faraday cup. The man-made spike <sup>205</sup>Pb was spiked in pg quantities as there is no natural <sup>205</sup>Pb and it could be measured in the gas ionization chamber. This work resulted in a method to determine <sup>210</sup>Pb by AMS, with a theoretical detection limit of ≤0.11 mBq at the new A.E Lalonde AMS facility

## Background

Radiometric techniques ( $\alpha$ , and  $\beta$  and  $\gamma$ -spectrometry) usually are used to quantify  $^{210}\text{Pb}$  (Hou & Roos 2008), table 1.  $^{210}\text{Pb}$  emits a weak B particle with an end point energy of 64 keV, which is difficult to detect, figure 2. Therefore,  $\alpha$  and  $\beta$ -spectrometry measurements of  $^{210}\text{Pb}$  are usually indirect because they measure the decay products of  $^{210}\text{Pb}$  ( $^{210}\text{Bi}$  and  $^{210}\text{Po}$ ). These measurements also require in-growth, sample preparation and counting times that can take days to months to achieve a useful analytical detection limit, table 1. On the other hand, high resolution (HPGe)  $\gamma$  spectrometry may be used to directly measure  $^{210}\text{Pb}$  using the 0.047 MeV gamma photon, figure 2. This technique requires little to no sample preparation but the detection limit is significantly higher than that of  $\alpha$  and  $\beta$  spectrometry (Hou & Roos 2008).

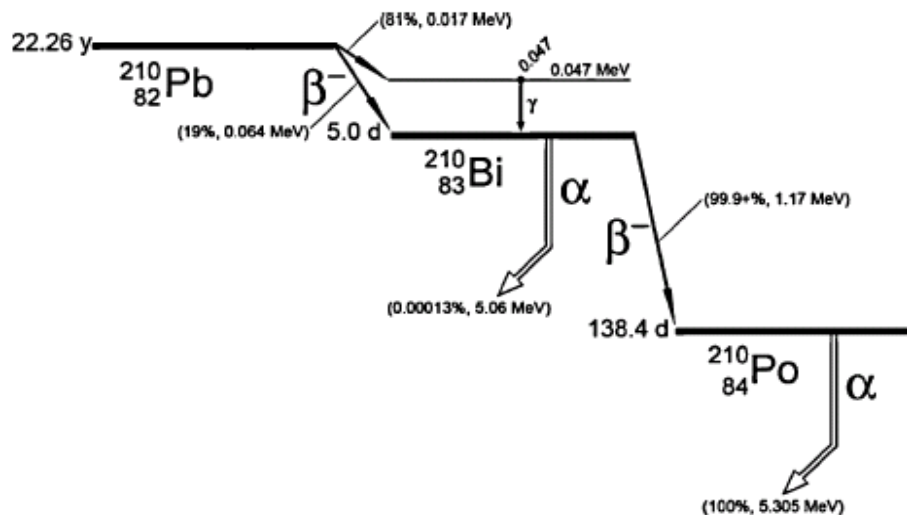


**Figure 2** Decay scheme for  $^{210}\text{Pb}$ . Image modified from Lariviere *et al.* 2006

Another technique to directly measure  $^{210}\text{Pb}$  is mass spectrometry. The field of mass spectrometry potentially offers a lower or comparable limit of detection to those of radiometric techniques. It does not require a period of in-growth to achieve secular equilibrium and it may require significantly less sample preparation. Previous studies have investigated Inductively Coupled

Plasma-Mass Spectroscopy (ICP-MS) and Collision Cell ICP-MS (CC ICP-MS) (Lariviere *et al.* 2006; Amr *et al.* 2010). Both techniques provide detection limits comparable to those of  $\gamma$ -spectrometry, table 1. They require more rigorous sample preparation to eliminate other elements from the sample that could form diatomic molecules with a mass of 210. They also suffer from abundance sensitivity issues since stable Pb is often present in the environment with concentrations more than  $10^9$  times higher than the concentrations of  $^{210}\text{Pb}$ .

Accelerator Mass Spectrometry (AMS) has been used in the past to study stable Pb (Middleton 1990; Zhao *et al.* 2010) and a proof of principal  $^{210}\text{Pb}$  detection was made by Steier et al (2002) but no detection limit nor do any in-depth studies exist on  $^{210}\text{Pb}$  determination by AMS. AMS has several potential advantages to measure  $^{210}\text{Pb}$  and it is compared to the other analytical techniques in more detail below.

#### *Accelerator Mass Spectrometry*

The AMS facility at IsoTrace was designed with two injection lines, figure 3. The first line using an SO-110 Source followed by the 1st  $90^\circ$  magnet which feeds in into a Isobar Separator for Anions (ISA). The second injection line, labelled 4 in figure 3, uses an 834 SIMS-type  $\text{Cs}^+$  sputter source, which connects a  $90^\circ$  magnet but does not use an ISA. All of the experiments performed at IsoTrace were done with the second injection line as our work did not require the ISA. All samples were loaded into a 834 SIMS-type  $\text{Cs}^+$  sputter source, the resulting molecular anions of Pb were selected by the 1st  $90^\circ$  magnet. The selected molecular anions were broken apart and the +3 charge state of Pb was selected by the second  $90^\circ$  magnet. The +3 charge state was used because it increases the probability of columbic explosion of molecular anions and the +1 and +2 charge of Pb could not be selected by the high energy magnetic. An Electrostatic analyzer (ESA) selected ions with appropriate energies, which were are then collected in Gas Ionization Chamber (GIC) detector.

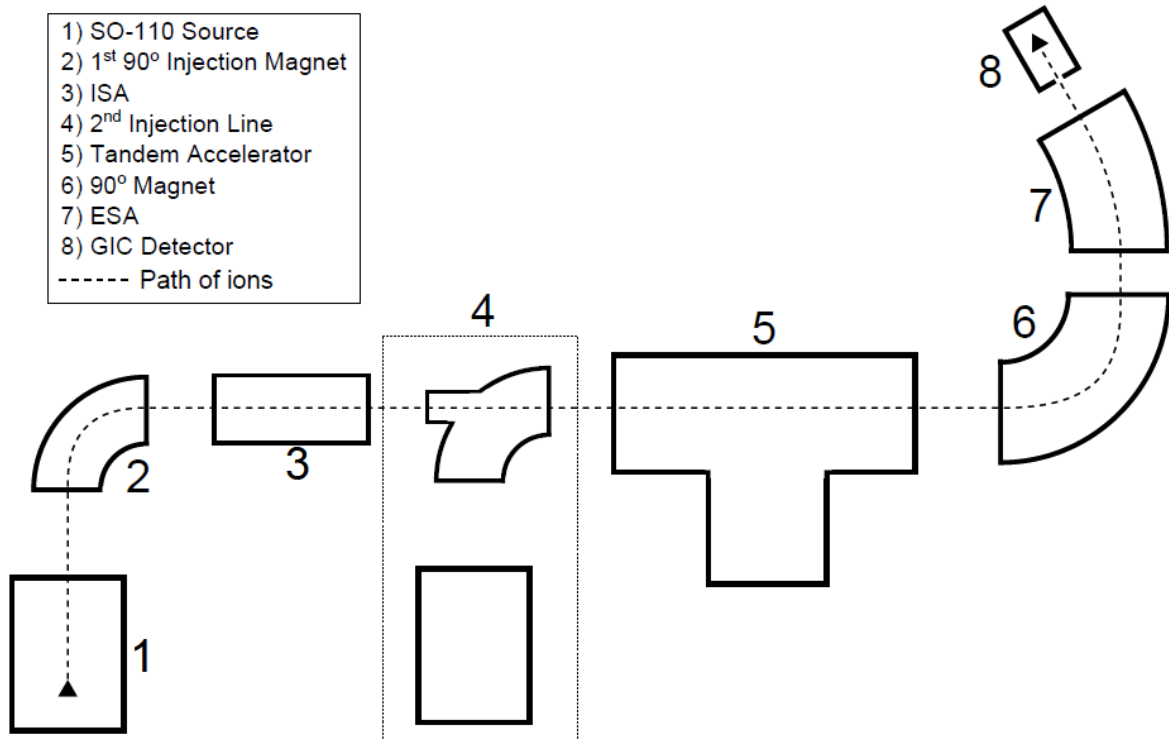


**Figure 3** Schematic of AMS at IsoTrace. Modified from MacDonald 2014

### *Alpha-spectroscopy*

The determination of  $^{210}\text{Pb}$  may be carried out through measurements of its decay product  $^{210}\text{Po}$ , a pure  $\alpha$  emitter, using  $\alpha$ -spectrometry (Ebaid & Khater 2006). The samples are normally decomposed and  $^{210}\text{Po}$  is removed from the matrix by solvent extraction or auto-deposited from the solution onto a stainless steel or a silver disk. This eliminates the  $^{210}\text{Po}$  from the solution, which might not be present in equal concentration with the  $^{210}\text{Pb}$ . Then the sample is stored for 3-6 months to allow for the in-growth of  $^{210}\text{Po}$  from the  $^{210}\text{Pb}$  in the sample and this  $^{210}\text{Po}$  is then deposited onto a stainless steel or silver disk and measured for 1000min by  $\alpha$  spectrometry using a semiconductor detector (Ebaid & Khater 2006; Hou & Roos 2008). This results in a detection limit of 0.1-1mBq of  $^{210}\text{Pb}$ . The low detection limit is a result of the very low background of the alpha spectrometer and

high counting efficiency between 20-40% (Vesterbacka & Ikäheimonen 2005). For this reason,  $\alpha$  spectrometry has been used for many measurements of environmental samples (Jia *et al.* 2000).

#### *Beta-spectrometry*

An alternative method for measuring  $^{210}\text{Pb}$  in environmental samples is  $\beta$ -spectrometry measurement of  $^{210}\text{Bi}$ , the daughter of  $^{210}\text{Pb}$ .  $\beta$ -spectrometry provides an alternative method to  $\alpha$  spectrometry as it shortens the in-growth period for secular equilibrium because  $^{210}\text{Bi}$  has a shorter half-life (Hou & Roos 2008). Samples for  $\beta$ -spectrometry are decomposed and Pb separated from the samples using ion or extraction chromatography. The Pb is then stored for 8-9 days to allow for in-growth of  $^{210}\text{Bi}$ . A limit of detection of 7 mBq for  $^{210}\text{Pb}$  has been cited with a count time of 1000min on a Liquid Scintillation Counter (LSC) (Brown 2005). However, interferences from  $^{210}\text{Pb}$  decays require a careful calibration of the detector to ensure accurate measurements of  $^{210}\text{Pb}$  using  $^{210}\text{Bi}$  by LSC.

The  $^{210}\text{Pb}$  decay series includes low energy  $\beta$  particles from  $^{210}\text{Pb}$  along with the higher energy  $\beta$  particles emitted from  $^{210}\text{Bi}$  and  $\alpha$  particles from  $^{210}\text{Po}$ , figure 2. This makes it is necessary to calibrate the LSC detector for reliable measurements of  $^{210}\text{Pb}$  (Ebaid & Khater 2006). There are some LSC that have simultaneous and separate determination of both  $\alpha$  and  $\beta$  events but this separation often is not always 100% efficient and therefore interferences must be evaluated and minimized. In addition, quenching may occur in LSC samples and this effect must be accounted for to ensure accurate measurements of  $^{210}\text{Pb}$  (Ebaid & Khater 2006).

#### *Gamma-spectrometry*

Unlike the other radiometric techniques,  $\gamma$ -spectrometry measures  $^{210}\text{Pb}$  directly. The direct measurement counts the 46.5keV photons emitted with an intensity of 4.0% of the decays of  $^{210}\text{Pb}$  (Hurtado *et al.* 2002). The low probability of the emission of  $\gamma$ -rays from  $^{210}\text{Pb}$  along with the low energy of the  $\gamma$ -ray, self absorption and interferences from other  $\gamma$ -X rays result in a detection limit of

440mBq when samples are counted for 1000min (Hou & Roos 2008). This detection limit of  $\gamma$  spectrometry is significantly higher than those reported for  $\alpha$  and  $\beta$  spectrometry. However, little to no sample preparation is required compared to other radiometric techniques as the  $^{210}\text{Pb}$  photon is measured directly. Nonetheless, due to a detection limit of 440mBq there are limited numbers of environmental applications for existing  $\gamma$  spectrometry techniques ((Ebaid & Khater 2006).

### *Mass spectrometry*

Inductively Coupled Plasma-Mass Spectroscopy (ICP-MS) has been assessed as a method to determine  $^{210}\text{Pb}$  (Lariviere *et al.* 2006). This technique is similar to  $\gamma$  spectrometry as it measures  $^{210}\text{Pb}$  directly. But rather than counting  $\gamma$ -rays from  $^{210}\text{Pb}$  decays, ICP-MS measures  $^{210}\text{Pb}$  ions. Hence, ICP-MS measurements suffer from molecular interferences of  $^{210}\text{Pb}$  such as  $^{209}\text{BiH}$ ,  $^{208}\text{PbH}_2$ ,  $^{194}\text{Pt}^{16}\text{O}$ ,  $^{198}\text{Hg}^{12}\text{C}$  and  $^{170}\text{Er}^{40}\text{Ar}$ . These interferences were removed by Lariviere *et al.* (2006) by directly introducing the volatile tetraethyl Pb compound to the plasma. However, due to abundance sensitivity or tailing from  $^{208}\text{Pb}$  a detection limit of 90mBq/L was reported (Lariviere *et al.* 2006). A collision cell ICP-MS was used to remove the tailing from stable Pb but a detection limit of 698Bq/L was reported (Amr *et al.* 2010). Further, with sample preparation requiring pre-concentration by evaporation or by co-precipitation followed by the use of Sr\*Spec resin to separate anions the overall time required for an ICP-MS measurement is two days (Lariviere *et al.* 2006). This makes ICP-MS a less attractive method compared to  $\gamma$  spectrometry as both techniques have similar detection limits but  $\gamma$  spectrometry requires no sample preparation (Hou & Roos 2008). An alternative approach to direct measurements of  $^{210}\text{Pb}$  is Accelerator Mass Spectrometer (AMS).

The measurement of  $^{210}\text{Pb}$  by AMS has approximately 10 times higher instrumental sensitivity compared to ICP-MS and several other potential advantages, but little literature exists on  $^{210}\text{Pb}$  measurements by AMS (Becker & Dietze 2003). These advantages of AMS include:

1. AMS has very good mass selection so that measurements with atom ratios of  $10^{-10}$  to  $10^{-15}$  can be made for many isotope pairs and thus the abundance sensitivity issue is eliminated.
2. AMS eliminates molecular interferences that have limited other mass spectrometry measurements.
3. AMS targets can be prepared using fluoride precipitation chemistry that has been developed for actinide chemistry (e.g. Kazi et al 2014)
4.  $^{210}\text{Pb}$ : $^{208}\text{Pb}$  atom ratios of  $10^{-12}$  are expected in people who are exposed to moderate concentrations of Rn in the indoor environment. The measurement of this ratio by AMS would be lower than the  $^{210}\text{Pb}$  detection limit of any other measurement technique
5. Measurements of atom ratios of  $10^{-12}$  have been made successfully for many radionuclides. It is reasonable to hypothesize that  $^{210}\text{Pb}$  measurements can be made by AMS in this range of concentration.

Stable Pb was tested in the sputter source by Middleton (1990) to determine the ability of Pb to form a negative atomic or molecular anion (a requirement of AMS). Middleton noted that Pb was one of the most frustrating compounds they measured because it did not readily produce a stable beam of anions from the cesium sputter source. Steier *et al.* (2002) tested measurements of  $^{210}\text{PbF}_3^-$  by AMS using a ratio of  $^{210}\text{Pb}/^{208}\text{Pb}$  of  $2 \times 10^{-8}$  when they demonstrated that heavy nuclides could be measured on a 'small' AMS machine. However, this concentration is too high to be useful in radon studies, no detection limit was reported and they did not explore ways to optimize the measurement (Steier *et al.* 2002). The production of a  $\text{PbF}_3^-$  ion beam in a sputter source was mentioned in a survey of molecular fluorides ( $\text{MF}_n^-$ ) demonstrating that  $\text{MF}_n^-$  generate large currents and may be used to eliminate

isobaric interferences (Zhao *et al.* 2010). The small but growing literature regarding  $^{210}\text{Pb}$  measurements by AMS warrants further investigation.

### *Summary*

$^{210}\text{Pb}$  is used in geochronology as it is part of the  $^{238}\text{U}$  decays series and in environmental health as it is the longest lived radioisotope after a series of decays of Rn, a natural occurring carcinogen (Rubin *et al.* 2005; Ladinskaya *et al.* 1973).  $^{210}\text{Pb}$  may be measured either by radiometric or mass spectrometry techniques. Radiometric techniques using  $\alpha$  and  $\beta$  spectrometry, offer low detections limits with long sample preparation and are the conventional techniques used for environmental samples of  $^{210}\text{Pb}$  (Jia *et al.* 2000; Hou & Roos 2008). Higher detections limits with little to no sample preparation can be achieved by  $\gamma$ -spectrometry. A similar detection limit to  $\gamma$ -spectrometry measurement of  $^{210}\text{Pb}$  is possible by ICP-MS. However, ICP-MS measurements of  $^{210}\text{Pb}$  suffer from abundance sensitivity of stable Pb and require a couple of days of sample preparation (Lariviere *et al.* 2006). A potential mass spectrometry alternative is AMS with its low detection limit and low abundance sensitivity. Stable Pb has been measured on an AMS by Middleton (1990) to determine the ability of Pb to form negative and molecular anions. Stable Pb was also mentioned in a survey of  $\text{MF}_n^-$  ions by AMS whereby Pb selectively formed  $\text{PbF}_3^-$  (Zhao *et al.* 2010).  $^{210}\text{PbF}_3^-$  was measured by Steier *et al.* (2002) on an AMS but no optimization of the  $^{210}\text{PbF}_3^-$  beam was attempted nor was a detection limit reported as the purpose of the study was to demonstrate that heavy nuclides could be measured by a ‘small’ AMS. Therefore,  $^{210}\text{Pb}$  measurement by AMS warrants further investigation.

### **Thesis Outline**

This thesis is presented as two manuscripts, both of which were written to address the two themes of this study. The first manuscript (Chapter 2) investigates the Pb chemistry in a  $\text{Cs}^+$  sputter source used

in AMS. The second manuscript (Chapter 3) investigates the use of  $^{204,205}$  &  $^{208}\text{Pb}$  spikes for the quantification of  $^{210}\text{Pb}$  by isotope dilution.

Chapter 2 focuses on the understanding the Pb chemistry in A  $\text{Cs}^+$  sputter in order to optimize the overall efficiency for  $^{210}\text{Pb}$  measurements by AMS. The manuscript will be submitted to Nuclear Instruments and Methods in Physics Research B.

Chapter 3 is a paper focusing on the evaluation of  $^{204,205}$  &  $^{208}\text{Pb}$  spikes for the quantification of  $^{210}\text{Pb}$  by AMS. The manuscript will be submitted to Rapid Communications in Mass Spectrometry

## References

AL-ZOUGHLOOL, M., & KREWSKI, D. 2009. Health effects of radon: a review of the literature.

*International journal of radiation biology.* **85**, 57-69.

AMR, M. A., AL-SAAD, K. A., & HELAL, A. I. 2010. Ultra-trace measurements of  $^{210}\text{Pb}$  in natural occurring radioactive materials by ICP-MS. *Nuclear Instruments and Methods in Physics Research Section A: Accelerators, Spectrometers, Detectors and Associated Equipment.* **615**, 237-241.

BECKER, J. S., & DIETZE, H. J. 2003. State-of-the-art in inorganic mass spectrometry for analysis of high-purity materials. *International Journal of Mass Spectrometry.* **228**, 127-150.

BEIR, V. I. 1999. Health effects of exposure to radon. *Committee on health risks of exposure to radon, Board on radiation effects research, Commission on life sciences, National Research Council.*

BROWN, S. A. 2005. Determination of  $^{210}\text{Po}$  and  $^{210}\text{Pb}$  in hydrometallurgical samples using liquid scintillation counting. *Journal of radioanalytical and nuclear chemistry.* **264**, 505-509.

MACDONALD, C. 2014. Master's thesis. University of Ottawa.

- DARBY, S., HILL, D., AUVINEN, A., BARROS-DIOS, J. M., BAYSSON, H., BOCHICCHIO, F. & DOLL, R. 2005. Radon in homes and risk of lung cancer: collaborative analysis of individual data from 13 European case-control studies. *Bmj.* **330**, 223.
- EBAID, Y. Y., & KHATER, A. E. M. 2006. Determination of  $^{210}\text{Pb}$  in environmental samples. *Journal of radioanalytical and nuclear chemistry.* **270**, 609-619.
- EISENBUD, M., LAURER, G. R., ROSEN, J. C., COHEN, N., & THOMAS, J. 1969. In vivo measurement of lead-210 as an indicator of cumulative radon daughter exposure in uranium miners. *Health physics.* **16**, 637-646.
- ERICKSON, B. E. 2007. Toxin or medicine? Explanatory models of radon in Montana health mines. *Medical anthropology quarterly.* **21**, 1-21.
- FALKENBACH, A. 2001. Combined radon and heat exposure for treatment of rheumatic diseases: a clinical approach. In *Thermotherapy for Neoplasia, Inflammation, and Pain* (pp. 495-503). Springer Japan.
- HOU, X., & ROOS, P. 2008. Critical comparison of radiometric and mass spectrometric methods for the determination of radionuclides in environmental, biological and nuclear waste samples. *Analytica Chimica Acta*, **608**, 105-139.
- HURTADO, S., GARCÍA-TENORIO, R., & GARCÍA-LEÓN, M. 2003.  $^{210}\text{Pb}$  determination in lead shields for low-level  $\gamma$ -spectrometry applying two independent radiometric techniques. *Nuclear Instruments and Methods in Physics Research Section A: Accelerators, Spectrometers, Detectors and Associated Equipment.* **497**, 381-388.
- JIA, G., BELLI, M., BLASI, M., MARCHETTI, A., ROSAMILIA, S., & SANSONE, U. 2000.  $^{210}\text{Pb}$  and  $^{210}\text{Po}$  determination in environmental samples. *Applied Radiation and Isotopes*, **53**, 115-120.

- KAZI, Z. H., CORNETT, J. R., ZHAO, X., & KIESER, L. 2014. Americium and plutonium separation by extraction chromatography for determination by accelerator mass spectrometry. *Analytica chimica acta*. **829**, 75-80.
- LADINSKAYA, L. A., PARFENOV, Y. D., POPOV, D. K., & FEDOROVA, A. V. 1973.  $^{210}\text{Pb}$  and  $^{210}\text{Po}$  content in air, water, foodstuffs, and the human body. *Archives of Environmental Health: An International Journal*. **27**, 254-258.
- LARIVIERE, D., TAYLOR, V. F., EVANS, R. D., & CORNETT, R. J. 2006. Radionuclide determination in environmental samples by inductively coupled plasma mass spectrometry. *Spectrochimica Acta Part B: Atomic Spectroscopy*. **61**, 877-904.
- MIDDLETON, R. A Negative-Ion Book, Dept. of Phys., Univ. of Pennsylvania, 1990, Available at a Brookhaven URL: <http://tvdg10.phy.bnl.gov/COOKBOOK/>
- OLDFIELD, F., & APPLEBY, P. G. 1984. Empirical testing of  $^{210}\text{Pb}$ -dating models for lake sediments. *Lake Sediments and Environmental History*. **15**, 93-123.
- OSTROWSKI, W. 1968. George Hevesy inventor of isotope methods in biochemical studies. *Postepy biochemii* **14**, 149–153.
- RICHARDSON, R. B., EATOUGH, J. P., & HENSHAW, D. L. 1991. Dose to red bone marrow from natural radon and thoron exposure. *The British journal of radiology*. **64**, 608-6
- RUBIN, K. H., VAN DER ZANDER, I., SMITH, M. C., & BERGMANIS, E. C. 2005. Minimum speed limit for ocean ridge magmatism from  $^{210}\text{Pb}$ – $^{226}\text{Ra}$ – $^{230}\text{Th}$  disequilibria. *Nature*. **437**, 534-538.
- STEIER, P., GOLSER, R., KUTSCHERA, W., LIECHTENSTEIN, V., PRILLER, A., VALENTA, A., & VOCKENHUBER, C. 2002. Heavy ion AMS with a “small” accelerator. *Nuclear Instruments and Methods in Physics Research Section B: Beam Interactions with Materials and Atoms*. **188**, 283-287.

- STEWART, B. W., & KLEIHUES, P. (Eds.). 2003. *World cancer report*. **57**. Lyon: IARC press.
- VESTERBACKA, P., & IKÄHEIMONEN, T. K. 2005. Optimization of  $^{210}\text{Pb}$  determination via spontaneous deposition of  $^{210}\text{Po}$  on a silver disk. *Analytica chimica acta*. **545** 252-261.
- WAHL, W., HANINGER, T., KUCHEIDA, D., ROTH, P., & PARETZKE, H. G. 2000. Study of long-term radon progeny in humans for retrospective evaluation of radon exposure. *Journal of Radioanalytical and Nuclear Chemistry*. **243**, 447-450
- WORLD HEALTH ORGANIZATION (Ed.). 2009. *WHO handbook on indoor radon: a public health perspective*. World Health Organization.
- ZHAO, X. L., LITHERLAND, A. E., ELIADES, J., KIESER, W. E., & LIU, Q. 2010. Studies of anions from sputtering I: Survey of  $\text{MF}_n^-$ . *Nuclear Instruments and Methods in Physics Research Section B: Beam Interactions with Materials and Atoms*. **268**, 807-811.
- ZIELINSKI, J. M., CARR, Z., KREWSKI, D., & REPACHOLI, M. 2006. World Health Organization's International Radon Project. *Journal of Toxicology and Environmental Health, Part A*. **69**, 759-769

## CHAPTER 2

### Article I. Production of Pb beams for $^{205,210}\text{Pb}$ analysis by AMS

Adam Sookdeo<sup>1\*</sup>, Jack Cornett<sup>1</sup>, Xiaolei Zhao<sup>2</sup>, William. E. Kieser<sup>2</sup>

To be submitted to Nuclear Instruments and Methods in Physics Research B.

### Production of Pb beams for $^{205,210}\text{Pb}$ analysis by AMS

Adam Sookdeo<sup>1\*</sup>, Jack Cornett<sup>1</sup>, Xiaolei Zhao<sup>2</sup>, William. E. Kieser<sup>2</sup>

<sup>1</sup>*Department of Earth Science University of Ottawa*

<sup>2</sup>*Department of Physics, University of Ottawa*

#### Abstract

The measurement of rare radioactive lead isotopes ( $^{205}\text{Pb}$  or  $^{210}\text{Pb}$ ) by AMS requires the production of strong Pb negative ion beams from the ion source. This paper summarizes results of tests of different target compositions on Pb beam currents. The strongest current of Pb from a survey of Pb molecular anions in a  $\text{Cs}^+$  sputter source was the superhalogen  $\text{PbF}_3^-$ . This target was composed of  $\text{PbF}_2$ ,  $\text{AgF}_2$  and  $\text{CsF}$ . Fluxing the target matrix of  $\text{PbF}_2$ ,  $\text{AgF}_2$  and  $\text{CsF}$  in concentrated HF increased the target homogeneity, stability and durability of the  $\text{PbF}_3^-$  beam. This process also increased the production of  $\text{PbF}_3^-$  anions from the ion source. The count rate of  $^{210}\text{Pb}$  was increased 20 fold by the addition of 240  $\mu\text{g}$  of  $\text{PbF}_2$  to the  $^{210}\text{Pb}$  targets. In an SO-110 ion source, higher average currents of  $^{208}\text{PbF}_3^-$  were generated with lower rather than higher  $\text{Cs}^+$  sputtering currents.

## 1. Introduction.

Molecular anions have been used to extend the applicability of Accelerator Mass Spectrometry (AMS) to produce ion beams of elements that do not easily form negative atomic ions. Molecular oxides anions can be used due to oxides stability in ion sources but often molecular negative ions suffer from isobaric interferences [1]. In recent years, superhalogens, namely molecular fluorides in which the metal atom is fully oxidized, have been studied because of the large currents of these anions and molecular fluorides show a large degree of isobar selectivity [1] because the molecular fluoride anions generated from the ion source have been shown to be element specific. Measurements of the oxide, fluoride or other molecular anions of Pb remain limited to a survey of  $\text{MF}_n^-$  [1] and to a brief discussion by Middleton [2]. Middleton noted that Pb was one of the most frustrating elements he measured. The molecular fluoride anion of  $^{210}\text{Pb}$ ,  $^{210}\text{PbF}_3^-$  was measured by AMS but no detection limit was reported as the purpose of that study was to demonstrate the capabilities of a small AMS [3]. In order to better understand Pb chemistry in the ion source and thus extend the applicability of AMS to trace measurements of  $^{210}\text{Pb}$ , a radioisotope important in both environmental health and geochronology, various molecular compounds of Pb and target chemistry were explored using the IsoTrace AMS and A.E Lalonde AMS systems.

## 2. Cs<sup>+</sup> sputtering on PbF<sub>2</sub> targets

In the 834 SIMS type Cs sputter AMS ion source atomic and molecular anions are ejected in the backward direction from a fraction of the energy carried by Cs<sup>+</sup> beams. The majority of the energy deposited by Cs<sup>+</sup> beams ends up as heat, which is highly concentrated on the target. A simulation suggested that within a duration of a picosecond a nanometer zone on a target can be heated up to well over 1000°C [4,5]. The deposition of this quantity of heat on PbF<sub>2</sub> targets instantly causes them to become electrically conductive in the ion source. This change in conductivity is associated with a phase change of the PbF<sub>2</sub> crystal from orthorhombic to cubic, which occurs in a range from 200-800°C. This phase change results in fluorine displacement from the crystal structure [6,7], which promotes interactions of fluorine atoms and anions with the rare radioisotope(s) in the target enabling the formation of molecular fluoride anions. The most stable molecular fluoride anions had one more fluorine atom than the usual stoichiometry of the compound e.g. PbF<sub>3</sub><sup>-</sup> [1]. These fluoride anions formed on the sputter target surface can be considered to belong to a class of materials referred as 'self-assembled materials', a term used in material sciences [8]. Hence, in past [4] and recent [9] experiments to measure PuF<sub>4</sub><sup>-</sup> anions, PuF<sub>3</sub> was co-precipitated in NdF<sub>3</sub> and mixed with PbF<sub>2</sub>. The unique property of PbF<sub>2</sub> fluorination assistance has been discussed in detail by Zhao et al [4] but no literature exists on how to increase the production of PbF<sub>3</sub><sup>-</sup> anions. And there is no in-depth study on PbX<sub>n</sub>Y<sub>m</sub> crystals, where X/Y is either F, O, S or N, and their relative ability to produce PbX<sub>n</sub>Y<sub>m</sub><sup>-</sup> anions from a Cs sputter source. Moreover, no literature exists on the pre-treatment of Pb targets before they are placed in a Cs<sup>+</sup> sputter source. This paper summarizes tests of Pb and <sup>210</sup>Pb beam production using PbF<sub>2</sub> and

PbX<sub>n</sub>Y<sub>m</sub> compounds with the IsoTrace AMS system initially, and later with the A. E. Lalonde AMS system.

### 3. Molecular Anions of Pb

Several Pb compounds and mixtures were tested on the 834 SIMS-type Cs<sup>+</sup> sputter source to determine and compare the relative currents generated from the molecular anions of <sup>208</sup>PbX<sub>n</sub>Y<sub>m</sub><sup>-</sup>, (table 2). The currents of the different anions are a measure of the relative ionization efficiency or how often a molecular anion forms; i.e., the larger the current the more readily such a molecular anion forms. For the first set of experiments, chemicals were mechanically mixed with a glass stir rod in clean Savillex containers. The targets were sputtered by a 10μA 17.5keV Cs<sup>+</sup> primary beam focused at φ0.5mm spot, for 30mins. No current was collected for the first five minutes to allow the current to stabilize then the currents were collected in a Faraday cup located after an Electrostatic Analyzer (ESA) before the tandem accelerator every five minutes for 25min. Table 2 and figure 4 present a set of measurements that illustrate the largest currents; those with the greatest current, and thus highest ionization efficiency, were of PbF<sub>3</sub><sup>-</sup>.

The strongest current of the superhalogen PbF<sub>3</sub><sup>-</sup> was generated when an abundant amount of fluorine donors were present such as CsF and AgF<sub>2</sub>. The uncertainty associated with these measurements is limited by the ammeter reading error of ±0.1 nA as there are no other sources of electrons near the masses measured. We also noticed that the fluorine anions react in a specific pattern. Fluorine anions react with a less electron rich molecule unless an abundant amount of fluorine anions are present. Then fluorine anions will show no bias towards electron rich or poor molecules and fluorine anions may even substitute for less

electronegative atoms/molecules. Hence, with the target composed of PbO, PbF<sub>2</sub> and AgF<sub>2</sub>, fluorine anions preferentially reacted with <sup>208</sup>PbO to form <sup>208</sup>PbOF<sup>-</sup> rather than <sup>208</sup>PbF<sub>2</sub> to form <sup>208</sup>PbF<sub>3</sub><sup>-</sup>, which led to a 4.3 times larger <sup>208</sup>PbOF<sup>-</sup> than <sup>208</sup>PbF<sub>3</sub><sup>-</sup> current. But when an additional fluorine source e.g. CsF was added to the same mixture, fluorine anions showed no bias and most likely substituted for oxygen atoms as the <sup>208</sup>PbF<sub>3</sub><sup>-</sup> current was 5.8 times larger than the <sup>208</sup>PbOF<sup>-</sup> current. Moreover, the less electronegative molecules of SCN were substituted for fluorine when the target was composed of Pb(SCN)<sub>2</sub> and AgF<sub>2</sub> as a <sup>208</sup>PbF<sub>3</sub><sup>-</sup> beam of 60nA was generated but no current of Pb(SCN)<sub>2</sub>F<sup>-</sup> was measured. The inherent reactivity of fluorine anions and large beam generated as PbF<sub>3</sub><sup>-</sup> suggest that this superhalogen may be used to measure trace amounts of Pb when an abundant amount of fluorine donors is packed in the target.

#### **4. Effect of the chemical compositions of PbF<sub>2</sub> in targets on <sup>208</sup>PbF<sub>3</sub><sup>-</sup> current**

The weight ratios of CsF and AgF<sub>2</sub> powders were varied in order to test for an optimal ratio that would generate the largest current of PbF<sub>3</sub><sup>-</sup> (table 3). However, changing the weight ratio of CsF and AgF<sub>2</sub> did not affect the current of <sup>208</sup>PbF<sub>3</sub><sup>-</sup>. For next set of experiments PbF<sub>2</sub>, CsF and AgF<sub>2</sub> powders were added by weight to clean Savillex containers and mechanically mixed with glass stir rods. Targets were then loaded on 834 SIMS-type Cs<sup>+</sup> sputter source at IsoTrace. The Cs<sup>+</sup> flux remained at 10μA but the extraction voltage was changed from 17.5keV to 22.5keV to produce the larger currents of <sup>208</sup>PbF<sub>3</sub><sup>-</sup>. The protocol used in previous experiments was employed again. The current of <sup>208</sup>PbF<sub>3</sub><sup>-</sup> was collected at 5min intervals for 15mintues in a Faraday cup after an ESA, once 5mins had passed to allow the current of <sup>208</sup>PbF<sub>3</sub><sup>-</sup> to stabilize. In order to compare the measurements to those done previously, the current of <sup>208</sup>PbF<sub>3</sub><sup>-</sup> that would be generated at 17.5keV was estimated to be

81.6% lower than at 22.5keV as dictated by the change in phase space (table 3). The  $^{208}\text{PbF}_3^-$  current was independent of the ratios of CsF and  $\text{AgF}_2$  tested in the experiment. This is consistent with the observation that both compounds are very good oxidizers [10-12].

Increasing the extraction voltage to 22.5keV from 17.5keV increased the  $^{208}\text{PbF}_3^-$  current. The increase in the  $^{208}\text{PbF}_3^-$  current was due to the change in phase space at a higher extraction voltage as the  $^{208}\text{PbF}_3^-$  current estimated at 17.5keV is similar to the measurement of  $\text{PbF}_2$ ,  $\text{AgF}_2$  and CsF in table I. Although, the ratios of  $\text{AgF}_2$  and CsF did not change the  $^{208}\text{PbF}_3^-$  current, we observed that the  $^{208}\text{PbF}_3^-$  current did change depending on whether the targets were chemically or mechanically mixed.

#### **5. Effect of mechanical mixing compared to chemically fluxing $\text{PbF}_2$ targets on $^{208}\text{PbF}_3^-$ current**

The  $\text{PbF}_2$  targets can be prepared by mechanical mixing or by refluxing the compounds in HF. In the IsoTrace operating procedure, targets packed with a fluorinating agent are mechanically mixed with a glass stir rod to ensure homogeneity of the target matrix [4]. We tested the hypothesis that targets with the same chemistry that are prepared by fluxing in concentrated HF would improve the homogeneity resulting in a better and more constant production of  $\text{PbF}_3^-$ . In the aforementioned set of experiments, 1-2mg of  $\text{PbF}_2$  were packed and mechanically mixed with fluorinating agents using a glass stir rod. In the set of experiments involving mechanically mixed or chemically fluxed in conc.  $\text{HF}_{(\text{aq})}$  for either six hours or overnight, 237 $\mu\text{g}$  of common  $\text{PbF}_2$  were used, which better simulates target preparation for trace measurements of  $^{210}\text{Pb}$ . The summary of results is compiled in table 4. The lower current of  $^{208}\text{PbF}_3^-$  is due to the lower concentration of Pb used for this set of

experiments. In the chemically fluxed targets, the distribution of  $\text{PbF}_2$  was likely more homogenous than mechanically mixing hence the larger currents of  $^{208}\text{PbF}_3^-$  for chemically fluxed targets compared to those that were mechanically mixed (table 4). Thus, when the target is sputtered by  $\text{Cs}^+$ ,  $\text{PbF}_2$  molecules are in closer proximity to fluorine donors, increasing the current by a factor of 1.3-1.5 of that from mechanical mixtures.

#### **6. Effect of the concentration of common $\text{PbF}_2$ ( $\mu\text{g}$ ) compared to $^{205}\text{PbF}_2$ ( $\text{pg}$ ) on $^{210}\text{Pb}$ count rate**

The trace amount of  $^{210}\text{Pb}$  in a target was ‘spiked’ with a known amount of a Pb isotope in order to quantify  $^{210}\text{Pb}$  using isotope dilution [13]. When we were determining whether  $^{205}\text{Pb}$  or common Pb would be a suitable spike we observed that the count of  $^{210}\text{Pb}^{+3}$  varied, depending on which spike was used (see figure 5). All targets were packed with equal parts by weight of  $\text{AgF}_2$  and  $\text{CsF}$ . The targets spiked with  $237\mu\text{g}$  of common  $\text{PbF}_2$ , generated 20 times more counts of  $^{210}\text{Pb}^{+3}$  than targets spiked with  $6.9\text{pg}$  of  $^{205}\text{PbF}_2$ . The difference in the  $^{210}\text{Pb}^{+3}$  count rate may be explained by the orthorhombic to cubic phase change of  $\text{PbF}_2$  at higher temperatures [1,5]. As mentioned previously, the structural change to a cubic crystal increases the electrical conductivity of the  $\text{PbF}_2$  crystals. If the quantity of  $\text{PbF}_2$  is sufficient in the target the entire target’s electrical conductivity increases, promoting the interactions between  $\text{PbF}_2$  and  $\text{CsF}$  and  $\text{AgF}_2$ . This results in an increase in the production of  $\text{PbF}_3^-$  anions and an increase in the  $^{210}\text{Pb}^{+3}$  counts. If little to no  $\text{PbF}_2$  is present in the targets the ionic conductivity of the target does not change and thus a lower count rate of  $^{210}\text{Pb}^{+3}$  would be expected. Besides  $\text{PbF}_2$  no other fluoride crystals exhibit a cubic phase change at higher temperatures that increases electrical conductivity [14-16].

Compounds of AgI, AgCl and AgBr show a similar phase change at higher temperatures [14], which increases the ionic conductivity of the matrix. If these materials were to be used with PbF<sub>2</sub> targets, Ag ions would compete against PbF<sub>2</sub> for F<sup>-</sup> anions, which would ultimately reduce the current generated by PbF<sub>3</sub><sup>-</sup> anions. Thus, it is essential that there be enough PbF<sub>2</sub> present to increase the ionic conductivity of the target matrix to increase the formation of PbF<sub>3</sub><sup>-</sup> anions.

### **7. Effect of Cs<sup>+</sup> flux on <sup>208</sup>PbF<sub>3</sub><sup>-</sup> current**

At the newly commissioned A.E. Lalonde AMS facility a SO-110 type Cs<sup>+</sup> source was installed this source design differs greatly from the 834 SIMS-type Cs<sup>+</sup> source at IsoTrace. The 834 SIMS-type Cs<sup>+</sup> source is a mini-probe in which the primary Cs<sup>+</sup> sputter beam is generated from a frit ionizer located away from the sputter target with little line of sight. In this case the hot frit surface contributes little radiation thermal energy to the sputter target, i.e. the energy brought to the target is solely by the primary Cs<sup>+</sup> sputter beam. In the SO-110 Cs<sup>+</sup> sputter source a hemispheric ionizer is located right in front of the sputter target. In this case the thermal energy directly brought onto the sputter target by radiation is typically on the same order of magnitude as the primary Cs<sup>+</sup> sputter beam. As the thermal energy brought to sputter targets on a SO-110 source was different from previous measurements done with the 834 SIMS-type Cs<sup>+</sup> source, we performed preliminary measurements manipulating the Cs<sup>+</sup> flux in order to better understand the role of thermal energy brought to sputter targets with respect to Pb measurements.

The Cs<sup>+</sup> beam on the SO-110 was initially run at the Cs<sup>+</sup> fluence that produces 50μA of <sup>12</sup>C<sup>-</sup> from graphite. By turning the Cs reservoir heater off and turning on the quick cool

system, which expands compressed air over the Cs reservoir and by allowing it to run overnight, the  $\text{Cs}^+$  flux was lowered by a factor of 10 as indicated by the drop in  $^{12}\text{C}^-$  current to  $5\mu\text{A}$ . By decreasing the  $\text{Cs}^+$  flux we discovered that the current of  $^{208}\text{PbF}_3^-$  was positively affected (see figure 6). This may occur because a  $\text{Cs}^+$  fluence that generates  $50\mu\text{A}$  of  $^{12}\text{C}^-$  causes F to degas more rapidly before it is able to react with the  $\text{PbF}_2$ , compared to a  $\text{Cs}^+$  fluence that generates  $5\mu\text{A}$  of  $^{12}\text{C}^-$ . Hence the current of  $^{208}\text{PbF}_3^-$  is larger and more consistent for targets run at a lower  $\text{Cs}^+$  flux. To our knowledge, this observation has not been reported before and it warrants further investigation.

## 8. Conclusions

The largest current from a survey of  $\text{PbXY}^-$  anions where X/Y is either F, O, S or N, was generated from the superhalogen  $\text{PbF}_3^-$ . The current of  $\text{PbF}_3^-$  can be increased by fluxing  $\text{PbF}_2$  with fluorinating agents. The best fluorinating agents found to date are a combination of  $\text{AgF}_2$  and  $\text{CsF}$ . The count rates of  $^{210}\text{Pb}$  were enhanced when  $^{208}\text{PbF}_2$  was added to the target to promote the formation of the trace analyte  $^{210}\text{PbF}_3^-$ . The formation of  $\text{PbF}_3^-$  was improved using a lower  $\text{Cs}^+$  fluence. Further investigation is required to understand the properties of  $\text{PbF}_3^-$  and the role the  $\text{Cs}^+$  fluence has on the ionization efficiency of  $\text{PbF}_3^-$ .

## Acknowledgements

Financial support from NSERC, Canada Research Chairs program and Canada Foundation for Innovation are gratefully recognized. We would also like to thank A.E. Litherland and C.R.J Charles for their valuable contributions to this project.

## References

- [1] X.-L. Zhao, A.E. Litherland, J. Eliades, W.E. Kieser, Q. Liu, Nucl. Instrum. Methods B 268 (2010) 807.
- [2] R. Middleton, A Negative-Ion Book, Dept. of Phys., Univ. of Pennsylvania, (1990)  
Available at a Brookhaven URL: <http://tvdg10.phy.bnl.gov/COOKBOOK/>
- [3] P. Steier, R. Golser, W. Kutschera, V. Liechtenstein, A. Priller, A. Valenta, C. Vockenhuber. Nucl. Instrum. Methods B 188 (2002) 283.
- [4] X.-L. Zhao, W.E. Kieser, X.Dai, N.D. Priest, S. Kramer-Tremblay J. Eliades, A.E. Litherland. Nucl. Instrum. Methods B 294 (2013) 356.
- [5] Th.J. Colla, H.M. Urbassek, Radiat. Eff. Defects Solids 142 (1997) 439.
- [6] J.H.Kennedy, M. Ronald, H. James. J. Electrochem. Soc. 120 (1973) 1441.
- [7] M.J. Castiglione, P.A. Madden. J. Phys. Cond. Matter 13(2001) 9963.
- [8] A.Kumar, H.A. Biebuyck, G.M. Whitesides. (1994) Langmuir 10 (1994) 1498.
- [9] Z.H. Kazi, J.R. Cornett, X.-L. Zhao, W.E. Kieser. Anal. Chim. Act. 829 (2014) 75.
- [10] G.A. Samara. J. Phys. Chem. Solids 40 (1979) 509.
- [11] P. Malinowski, Z. Mazej, W. Grochala. Zeitschr. Anorgan. Allgem. Chemie, 634 (2008) 2608.
- [12] W.Grochala. J. Fluorine Chem129 (2009) 82.
- [13] R. Steele., J.S. Wall, R.C. De Bodo, N. Altszuler. Am J Physiol. 187 (1956) 15.
- [14] J.A. Wilkinson. Chem. Rev. 92 (1992) 505.
- [15] F. Zimmer, P. Ballone, M. Parrinello, J. Maier. Solid State Ionics 127 (2000) 277.
- [16] G.A. Samara. Phys. Rev. B 13 (1976) 4529.

**Table 2** Ratios of PbXY<sup>-</sup> compounds mixed with fluorinating agents or Ag and currents that they yielded on the 834 SIMS type ion source at IsoTrace.

Target composition	Ratio by weight	Average <sup>208</sup> Pb molecular anion current (nA)	Molecular anions
PbF <sub>2</sub> + AgF <sub>2</sub>	1 : 1	75	<sup>208</sup> PbF <sub>3</sub> <sup>-</sup>
PbF <sub>2</sub> + AgF <sub>2</sub> + CsF	9 : 6 : 10	175	<sup>208</sup> PbF <sub>3</sub> <sup>-</sup>
PbO + AgF <sub>2</sub>	3 : 5	63	<sup>208</sup> PbOF <sup>-</sup>
PbO + PbF <sub>2</sub>	3 : 5	23, 53 <sup>a</sup>	<sup>208</sup> PbF <sub>3</sub> <sup>-</sup> , <sup>208</sup> PbOF <sup>-</sup>
PbO + PbF <sub>2</sub> + AgF <sub>2</sub>	4 : 5 : 3	27.5, 120 <sup>a</sup>	<sup>208</sup> PbF <sub>3</sub> <sup>-</sup> , <sup>208</sup> PbOF <sup>-</sup>
PbO + PbF <sub>2</sub> + AgF <sub>2</sub> + CsF	5 : 5 : 4 : 4	145, 25 <sup>a</sup>	<sup>208</sup> PbF <sub>3</sub> <sup>-</sup> , <sup>208</sup> PbOF <sup>-</sup>
Pb(SCN) <sub>2</sub> + Ag	2 : 3	0.6	<sup>208</sup> Pb(SCN) <sub>2</sub> <sup>-</sup>
Pb(SCN) <sub>2</sub> + AgF <sub>2</sub>	7 : 6	60	<sup>208</sup> PbF <sub>3</sub> <sup>-</sup>
Pb(NO <sub>2</sub> ) <sub>2</sub> + Ag	5 : 2	0	-
PbSO <sub>4</sub> + Ag	4 : 5	4	<sup>208</sup> PbO <sub>2</sub> <sup>-</sup> & <sup>208</sup> PbS <sup>-</sup>
PbCO <sub>3</sub> + Ag	5 : 8	12.5	<sup>208</sup> PbO <sub>2</sub>

<sup>a</sup>Currents of <sup>208</sup>PbOF<sup>-</sup>

**Table 3** Current of  $^{208}\text{PbF}_3^-$  generated from targets composed with different ratios by weight of  $\text{PbF}_2$ :  $\text{AgF}_2$  and  $\text{CsF}$ .

Target	Ratio by weight	Average $^{208}\text{PbF}_3^-$ current at 22.5keV (nA)	Average $^{208}\text{PbF}_3^-$ current converted to 17keV (nA)
1	1:2:4	210	172
2	1:4:2	215	175
3	1:6:6	208	170

**Table 4**  $^{208}\text{PbF}_3^-$  currents from targets composed of 0.2mg of Pb and equal parts of  $\text{AgF}_2$  and  $\text{CsF}$ . Currents of  $\text{PbF}_3^-$  were collected after ESA-1 and measured 10mins after an initial 5min of  $\text{Cs}^+$  sputter.

Target	Mechanical (M) or Fluxed in conc. HF(F)	Flux time	Average $^{208}\text{PbF}_3^-$ current at 22.5keV (nA)
A	M	-	31
B	M	-	28
C	F	6hr	41
D	F	6hr	44
E	F	Overnight	40
F	F	Overnight	42

### List of figures

**Figure 4**  $^{208}\text{PbXY}^-$  currents from different chemical mixtures.

**Figure 5**  $^{210}\text{Pb}$  counts for targets with 1Bq of  $^{210}\text{Pb}$  spiked with either 5.4pg of  $^{205}\text{Pb}$  or 200 $\mu\text{g}$  of common Pb. All targets were packed with equal parts by weight of CsF and AgF<sub>2</sub>. The number of counts recorded in each experiment is shown above the bar.

**Figure 6**  $^{208}\text{PbF}_3^-$  current generated at different Cs<sup>+</sup> fluxes from pure PbF<sub>2</sub> targets using the SO-110 ion source at the Lalonde AMS Lab.

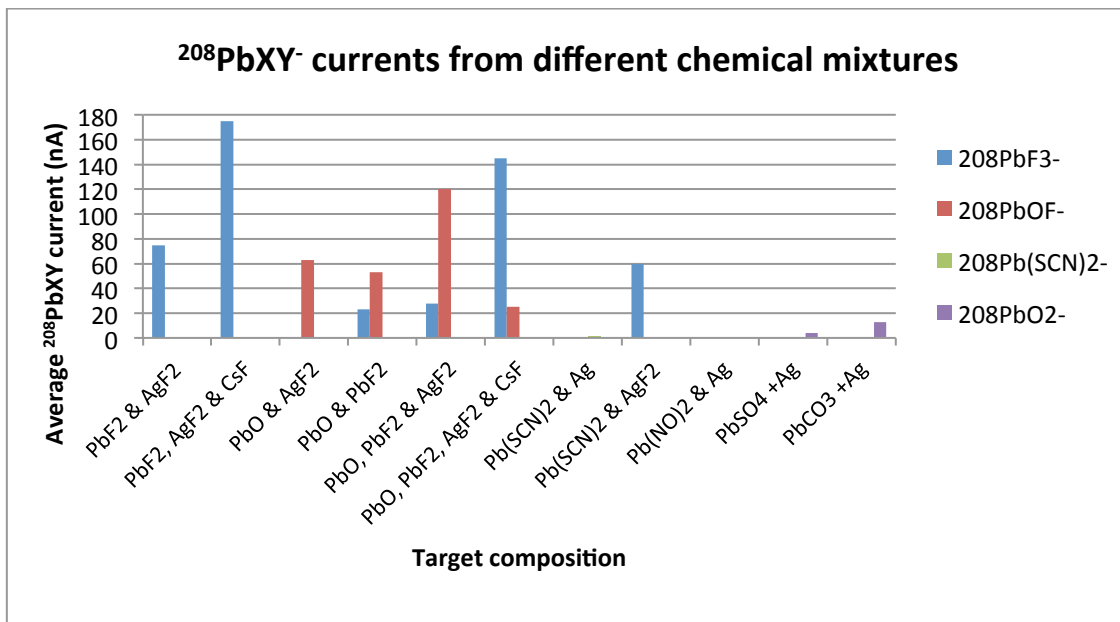


**Figure 4**

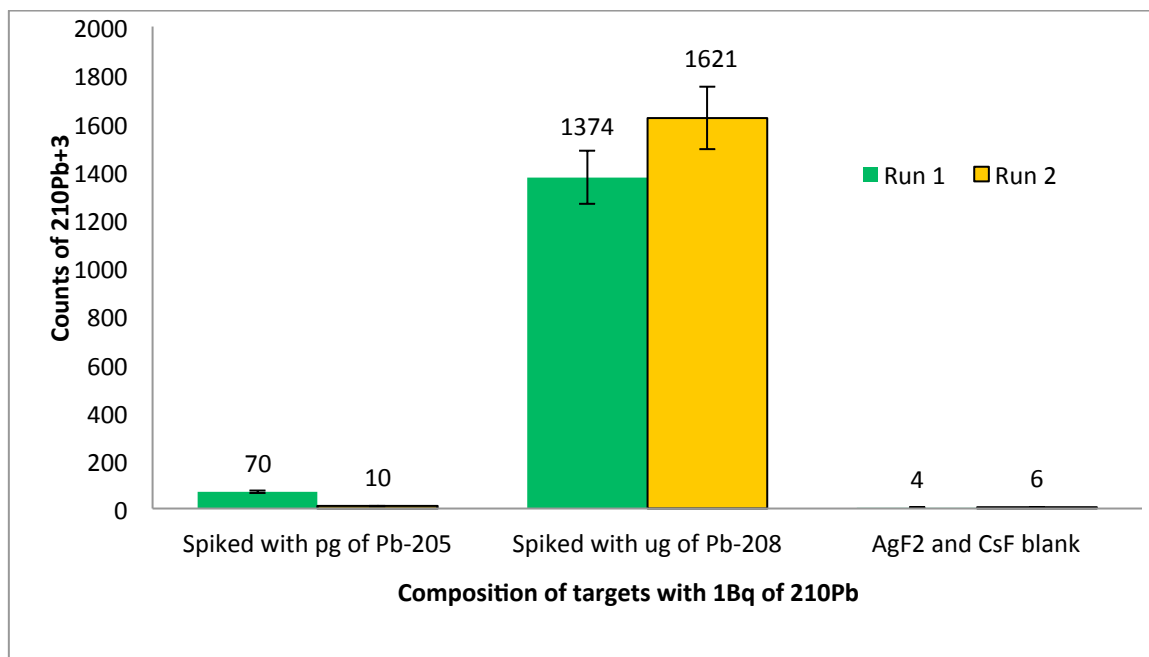


**Figure 5**

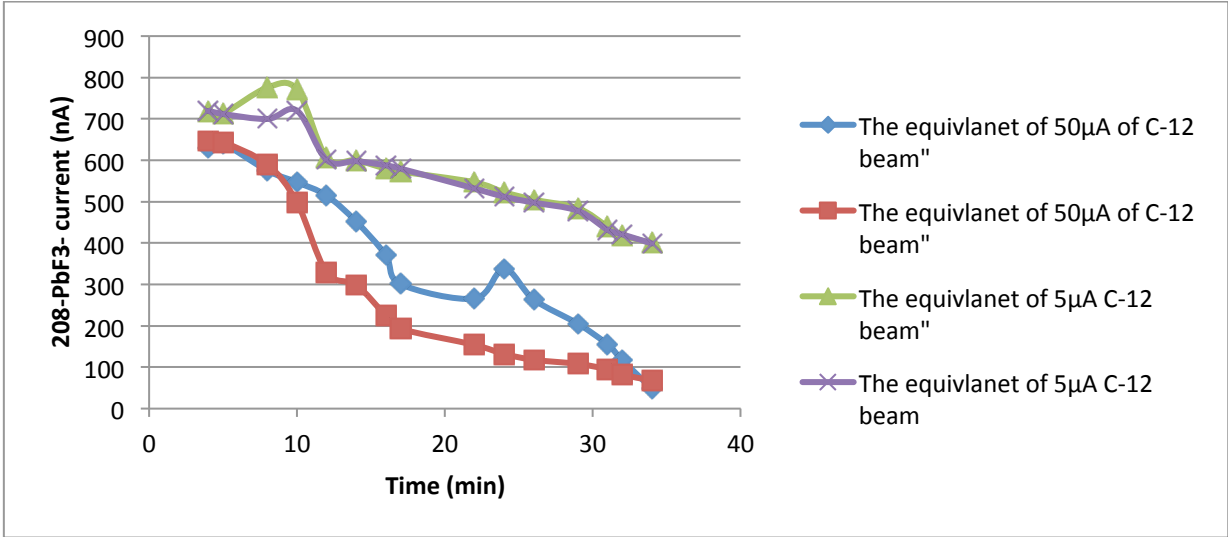


Figure 6

## CHAPTER 3

### Article II. Quantifying $^{210}\text{Pb}$ by Accelerator Mass Spectroscopy: A study of molecular and isobaric interferences of $^{204, 205, 208}\text{Pb}$ and $^{210}\text{Pb}$

A. Sookdeo<sup>1\*</sup>, J. Cornett<sup>1</sup>, X.L. Zhao<sup>2</sup>, C.R.J Charles<sup>2</sup>, & W. E. Keiser<sup>2</sup>

To be submitted to Rapid Communications in Mass Spectrometry.

### Quantifying $^{210}\text{Pb}$ by Accelerator Mass Spectroscopy: A study of molecular and isobaric interferences of $^{204, 205, 208}\text{Pb}$ and $^{210}\text{Pb}$

A. Sookdeo<sup>1\*</sup>, J. Cornett<sup>1</sup>, X.L. Zhao<sup>2</sup>, C.R.J Charles<sup>2</sup>, & W. E. Keiser<sup>2</sup>

<sup>1</sup>*Department of Earth Science University of Ottawa*

<sup>2</sup>*Department of Physics, University of Ottawa*

#### -ABSTRACT-

**RATIONALE:**  $^{210}\text{Pb}$  is an isotope that can provide lung cancer risk assessments from radon exposure in humans. Since the existing techniques for the determination of  $^{210}\text{Pb}$  cannot accomplish this due to detection limits, here we present a new method to determine low mBq of  $^{210}\text{Pb}$  by Accelerator Mass Spectrometry (AMS).

**METHODS:** AMS targets were prepared from our stock solutions of  $^{204}\text{Pb}$ ,  $^{205}\text{Pb}$ , and a stock solution of Pb to spike with  $^{208}\text{Pb}$  and stock solutions of  $^{210}\text{Pb}$ . All targets were measured using an 834 SIMS-type Cs<sup>+</sup> sputter source on 3MV tandem AMS.

**RESULTS:**  $^{204}\text{Pb}$  and  $^{205}\text{Pb}$  suffer from molecular and isobaric interferences that cannot be removed without sacrificing the efficiency of  $^{210}\text{Pb}$  measurements.  $^{208}\text{Pb}$  suffers from no interferences and targets spiked with  $^{208}\text{Pb}$  were below the abundance sensitivity of  $^{210}\text{Pb}/^{208}\text{Pb}$  of  $1.3 \times 10^{-12}$ . A detection limit of 4.4mBq and theoretical detection limit of  $\leq 0.11\text{mBq}$  of  $^{210}\text{Pb}$  were calculated for the IsoTrace facility and the A.E Lalonde facility, respectively.

**CONCLUSIONS:** This result advances the possibility of using AMS to detect mBq of  $^{210}\text{Pb}$ .

## Introduction

$^{210}\text{Pb}$  is a short-lived radioisotope (22.3 years half-life<sup>[1]</sup>) and belongs to the uranium decay series. It is the longest lived radioisotope after a series of decays from  $^{222}\text{Rn}$  and thus  $^{210}\text{Pb}$  has been used in fields of geochronology<sup>[1,2]</sup> and environmental health.<sup>[3]</sup> The determination of  $^{210}\text{Pb}$  has been done with Inductively Coupled Plasma-Mass Spectroscopy<sup>[4,5]</sup> (ICP-MS), Collision Cell ICP-MS<sup>[6]</sup> (CC ICP-MS) and more commonly  $\alpha$ ,  $\beta$ , and  $\gamma$  spectroscopy.<sup>[5]</sup> The lowest detection limit of ICP-MS reported was 90 mBq/L and for CC ICP-MS it was 688 mBq/L. For all radiometric techniques, the emissions from  $^{210}\text{Pb}$  decays are measured.<sup>[5,7]</sup> The lowest detection limit of all radiometric techniques is reached when  $^{210}\text{Po}$ , a decay product of  $^{210}\text{Pb}$  is allowed to accumulate in a sample as  $^{210}\text{Pb}$  decays and then  $^{210}\text{Po}$  is measured by  $\alpha$  spectroscopy (0.1-1mBq).<sup>[5,7]</sup> However, quantification of  $^{210}\text{Pb}$  for a single target with this low activity requires several days of acquisition time and often 3-5 months are required to allow for the in-growth of  $^{210}\text{Po}$ .<sup>[7]</sup> Also, a detection limit of 0.1-1mBq is too high to determine  $^{210}\text{Pb}$  in urine, bone and tissue samples in people exposed to moderate concentrations of  $^{222}\text{Rn}$ .<sup>[8]</sup> However, determining  $^{210}\text{Pb}$  in people exposed could provide critical information on radon exposure.<sup>[8]</sup> Furthermore, few measurements of  $^{210}\text{Pb}$  in arctic sediments have been done as the concentration in arctic fall below concentrations 0.1-1mBq of  $^{210}\text{Pb}$ .<sup>[9,10]</sup> The determination of  $^{210}\text{Pb}$  in arctic sediments that could better our understanding of sedimentation rates in the arctic.<sup>[10]</sup> There is the potential to measure  $^{210}\text{Pb}$  using AMS in these materials and thus provide new information for geochronology and environmental health. This work takes advantage of the properties of the  $\text{PbF}_3^-$  superhalogen anion<sup>[10,11]</sup> so that large currents of  $\text{PbF}_3^-$  can be produced in a  $\text{Cs}^+$  sputter source and thus  $^{210}\text{Pb}$  can be measured at low levels by Accelerator Mass Spectrometry (AMS), a analytical tool known for its low detection limits of radioisotopes.<sup>[11,12,13]</sup>

The formation efficiency of the superhalogen  $\text{PbF}_3^-$  in a  $\text{Cs}^+$  sputter source has recently been reported by our lab group and offers a promising way to detect  $^{210}\text{Pb}$ , but no studies to date have discussed the quantification of  $^{210}\text{Pb}$  by AMS.<sup>[14]</sup> Commonly, there are two ways to quantify rare

radioisotopes isotopes with AMS; either (1) measure the natural abundance of an isotopes in the target and compare this measurement to a standard curve or (2) 'spike' the target with a known amount of an isotope and calculate the amount of the rare radioisotope in the sample using isotope dilution. For the determination of  $^{210}\text{Pb}$ , the first approach requires the target to naturally contain either  $\mu\text{g}$  of Pb to measure a current of a stable Pb isotope in a Faraday cup or less than pg quantities of the isotope to measure counts in a gas ionization chamber. The second technique controls the amount of Pb isotope used to spike the target; either  $\mu\text{g}$  or pg quantities depending on the Pb isotope used. In this report, we discuss isotopes of Pb that can be used as spikes and their associated interferences as well as preliminary measurements of  $^{210}\text{Pb}$  spiked with  $^{208}\text{Pb}$ .

## **EXPERIMENTAL**

All AMS samples were made from our stock solutions of Pb isotopes, after several steps solids of  $\text{PbF}_2$  with equal parts by weight of  $\text{AgF}_2$  and  $\text{CsF}$  were packed into stainless steel target holders. The Ag1x8 resin was chosen for its capabilities to selectively retain Pb, while removing unwanted atoms.<sup>[15,16,17]</sup>

$^{204}\text{Pb}$  samples were prepared from our stock solution of 100ppm.  $^{205}\text{Pb}$  samples were prepared using our stock solution of 1.8pg/ $\mu\text{l}$  of the Parrish and Krogh stock.<sup>[18]</sup> Targets containing  $^{210}\text{Pb}$  were prepared either using our 8.62Bq stock of  $^{210}\text{Pb}$  or 100mg (66mBq of  $^{210}\text{Pb}$ ) of the standard reference material, CLV-1.<sup>[19]</sup> CLV-1 samples were previously digested in 5ml of concentrated  $\text{HNO}_3$ . All solutions were aliquoted to clean 7mL PFA Teflon Savillex containers and were evaporated to dryness on a hotplate at 120°C overnight. Targets not treated with Ag1x8 resin were dissolved in 1mL of concentrated  $\text{HF}_{(l)}$  and evaporated to dryness on a hotplate at 120°C overnight. Another 1ml of concentrated  $\text{HF}_{(l)}$  were added to these targets along with powders of either  $\text{AgF}_2$  or  $\text{AgF}_2$  and  $\text{CsF}$  in equal parts by weight. The lids were placed on the Savillex containers and the targets were fluxed overnight and after evaporated to dryness on a hotplate at 120°C.

Targets that were to be passed through an Ag1x8 resin to remove, interferences of Tl, Zn and Ce<sup>[15,16, 17]</sup> were dissolved in 1mL of concentrated HBr<sub>(l)</sub> and evaporated to dryness on a hotplate at 120°C. Then 0.5ml of 1.5N HBr<sub>(l)</sub> was added to the Savillex containers. The samples were then passed through Bio-Rad polyprep columns that were packed with 0.4ml of Ag1x8 resin previously conditioned with 1.5N HBr<sub>(l)</sub>. The columns were then washed twice with 2ml of 1.5N HBr<sub>(l)</sub>, and washed twice with 1ml of 3.2N HCl<sub>(l)</sub> to eliminate Ce. Pb was eluted from the column with 4mL of 6.2N HCl<sub>(l)</sub> added and collected in clean 7mL PFA Teflon Savillex containers. The purified Pb concentrate of Pb was evaporated to dryness on a hotplate overnight at 120°C and then 0.5ml of concentrated HF<sub>(l)</sub> was added. The solutions were dried again, 0.5mL of concentrated HF<sub>(l)</sub> along with powders of AgF<sub>2</sub> and CsF in equal parts by weight were added to the containers. The lids were placed on the Savillex containers and they were fluxed overnight at 120°C. Then the lids were removed and the solutions were dried.

The measurements were all performed at the IsoTrace Laboratory using an 3 MV tandem accelerator mass spectrometer.<sup>[20, 21]</sup> Approximately 30mg of samples were loaded into stainless targets holders and measured on an 834-SIMS type Cs<sup>+</sup> sputter source at 15keV extraction voltage with 10μA of Cs<sup>+</sup>, using a single spot method, unless specified otherwise. PbF<sub>3</sub><sup>-</sup> beams were extracted from the ion source and injected into the tandem accelerator.<sup>204, 205, 208 & 210</sup> PbF<sub>3</sub><sup>-</sup> were injected into the accelerator and the +3 charges were selected for analysis. In order to bend <sup>210</sup>Pb<sup>+3</sup> in the post accelerator magnetic analyzer, the terminal voltage was limited to 0.9600MV. <sup>205</sup>Pb<sup>+3</sup> and <sup>210</sup>Pb<sup>+3</sup> counts were collected in a gas ionization chamber. Currents of <sup>204</sup>Pb<sup>+3</sup> and <sup>208</sup>Pb<sup>+3</sup> were collected in an off axis Faraday cup at the focal plane of the post accelerator magnetic analyzer.

## RESULTS AND DISCUSSION

Table 5 shows that for each isotope of Pb there are interferences from a combination of atoms and molecules. These interferences if not reduced could ruin any measurements of a Pb isotope. <sup>204</sup>Pb is

present in all samples as it's primordial<sup>[22]</sup>. To swamp out any naturally variability in samples 250µg of  $^{204}\text{Pb}$  was used when preparing targets spiked with  $^{204}\text{Pb}$ . After  $^{204}\text{PbF}_3^-$  anions are injected into the AMS, the final product,  $^{204}\text{Pb}^{+3}$  is measured in a Faraday cup. Measurement of  $^{204}\text{Pb}^{+3}$  suffers from interference of  $^{68}\text{Zn}^{+1}$  that could come from molecular ions made up of trimers of  $^{68}\text{Zn}$  and  $^{57}\text{Fe}$ , i.e.  $(^{68}\text{Zn}_3)^{57}\text{Fe}^-$ , where  $^{57}\text{Fe}$  is from stainless targets holders. To ensure that all the material in a target is used a 16 spot raster method was adopted, figure 7. This technique moves the  $\text{Cs}^+$  sputter beam closer to the stainless steel target holder, potentially promoting the formation of  $(^{68}\text{Zn}_3)^{57}\text{Fe}^-$  anions. These anions are subsequently injected into the AMS by the low energy magnet, increasing the probability of  $^{68}\text{Zn}^{+1}$  ions entering the Faraday cup, affecting the accuracy  $^{204}\text{Pb}^{+3}$  measurement. To test that the  $^{57}\text{Fe}$  was coming from the interactions of the  $\text{Cs}^+$  sputter beam and the stainless steel targets holder, a single spot method was adopted, figure 6.

The effect of the  $\text{Cs}^+$  sputter beam on the formation of  $(^{68}\text{Zn}_3)^{57}\text{Fe}^-$  may be seen by the large increase in  $^{204}\text{Pb}^{+3}$  current when a single spot method was changed to a 16 spot method, figure 8. But as the chemistry of the ion source is not well understood there may be other possibilities for the increase that have yet to be understood. <sup>[23]</sup>

**Table 5** Mass-to-charge interferences for Pb isotopes.

Pb isotope	Mass-to-charge interference(s) selected by the injection magnetic	Mass-to-charge interference(s) in final detector
$^{204}\text{Pb}^a$	$(^{68}\text{Zn}_3)^{57}\text{Fe}^-$	$^{68}\text{Zn}^{+1}$
$^{205}\text{Pb}^b$	$^{205}\text{TlF}_3^-$ , $^{68}\text{Zn}^{137}\text{BaF}_3^-$ , $^{68}\text{Zn}^{137}\text{Ba}^{57}\text{Fe}^-$	$^{68}\text{Zn}^{+1}$ , $^{137}\text{Ba}^{+2}$ , $^{205}\text{Tl}^{+3}$
$^{208}\text{Pb}^a$	-	-
$^{210}\text{Pb}^b$	$^{70}\text{Zn}^{140}\text{CeF}_3^-$ , $^{70}\text{Zn}^{140}\text{Ce}^{57}\text{Fe}^-$	$^{70}\text{Zn}^{+1}$ , $^{140}\text{Ce}^{+2}$

<sup>a</sup>Collected in a Faraday cup

<sup>b</sup>Collected in a gas ionization chamber

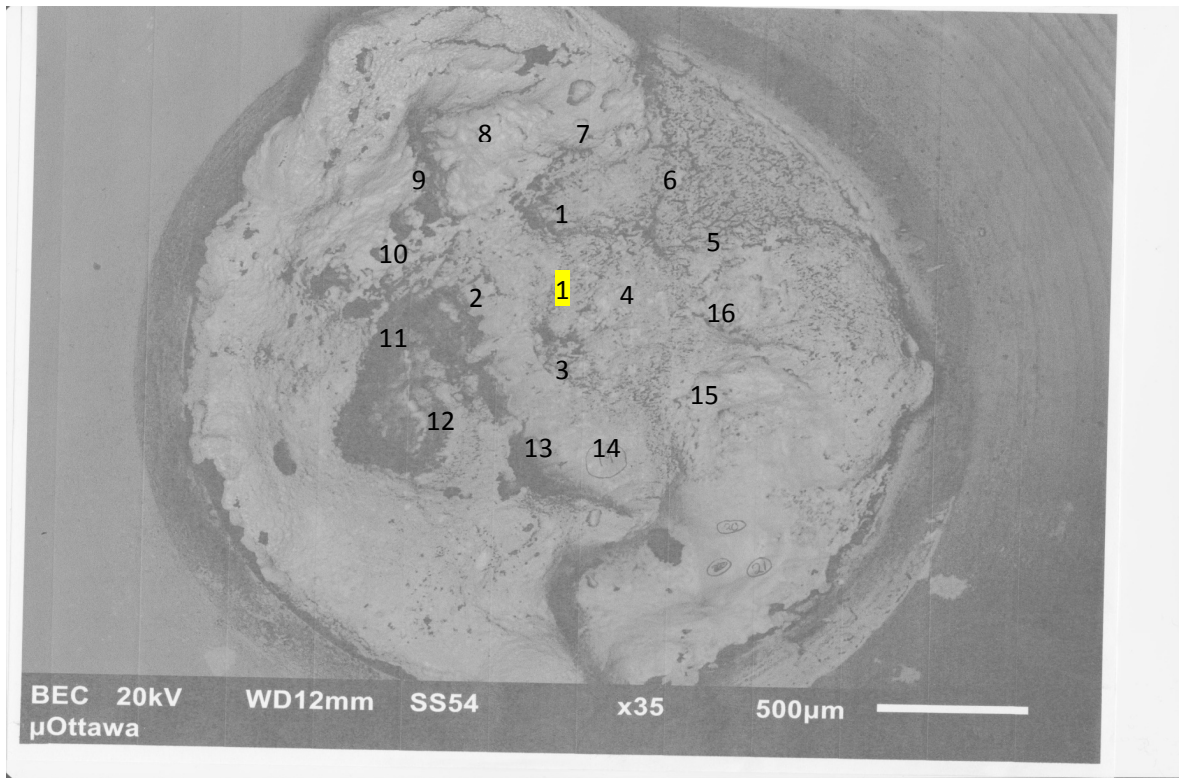


**Figure 7** An SEM image of a Pb target after Cs<sup>+</sup> sputtering. The highlighted 1 indicates the single spot method while the un-highlighted numbers indicated the location of Cs sputtering using a 16 spot method.

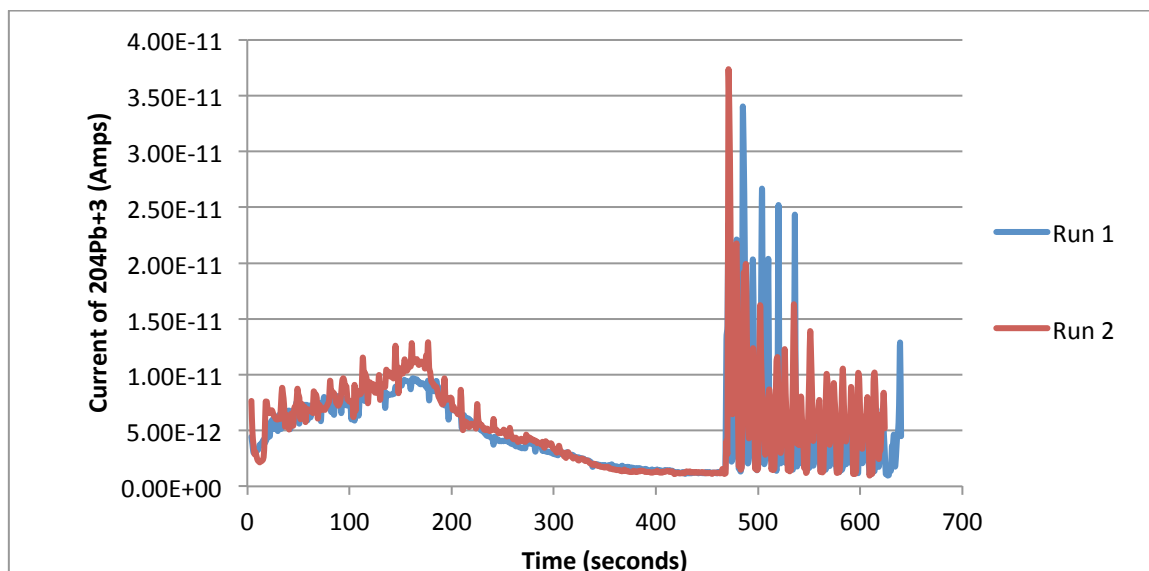


**Figure 8** Current measurements of  $^{204}\text{Pb}^{+3}$  for targets spiked with  $250\mu\text{g}$  of  $^{204}\text{Pb}$ . The  $\text{Cs}^+$  sputter source was changed from a single spot method to 16 spot method at 475seconds.

$^{204}\text{Pb}$  is only a suitable spike for trace measurements of  $^{210}\text{Pb}$  using target holders that contain no iron and/or using a single spot method to avoid the formation of  $(^{68}\text{Zn}_3)^{57}\text{Fe}^-$ . If a single spot is used this means much of target has to remain unused.

$^{205}\text{Pb}$  is a man-made isotope,<sup>[18]</sup> hence, in practice much smaller quantities (pico or femto grams) can be used for isotope dilution measurements of  $^{210}\text{Pb}$ . However,  $^{205}\text{Pb}$  suffers from  $^{205}\text{Tl}$  interference, table 5. Tests demonstrated that the majority of  $^{205}\text{Tl}$  interferences come from  $\text{CsF}$ , one of the fluorinating agents used to produce the  $\text{PbF}_3^-$  beam, figure 9. Targets using  $\text{CsF}$  increased the  $^{205}\text{Tl}$  count rate at mass 205 by about 1000 compared to samples that contained  $\text{AgF}_2$  and no  $\text{CsF}$ , figure 8. Although the  $\text{CsF}$  used in our experiments was 99.9% pure on a trace metal basis, we were unable to eliminate the isobaric interference from  $^{205}\text{Tl}$ . As a result,  $\text{CsF}$  cannot be used with targets that contain a  $^{205}\text{Pb}$  spike. However, it has been shown that when a target of  $\text{PbF}_2$  is packed with  $\text{AgF}_2$  in the absence of  $\text{CsF}$  an average current of  $\text{PbF}_3^-$  was 2.3 times lower than if mixture  $\text{CsF}$  was present.<sup>[14]</sup> Thus, using  $^{205}\text{Pb}$  spike with the absence of  $\text{CsF}$  decreases our detection by a factor of greater than 2.

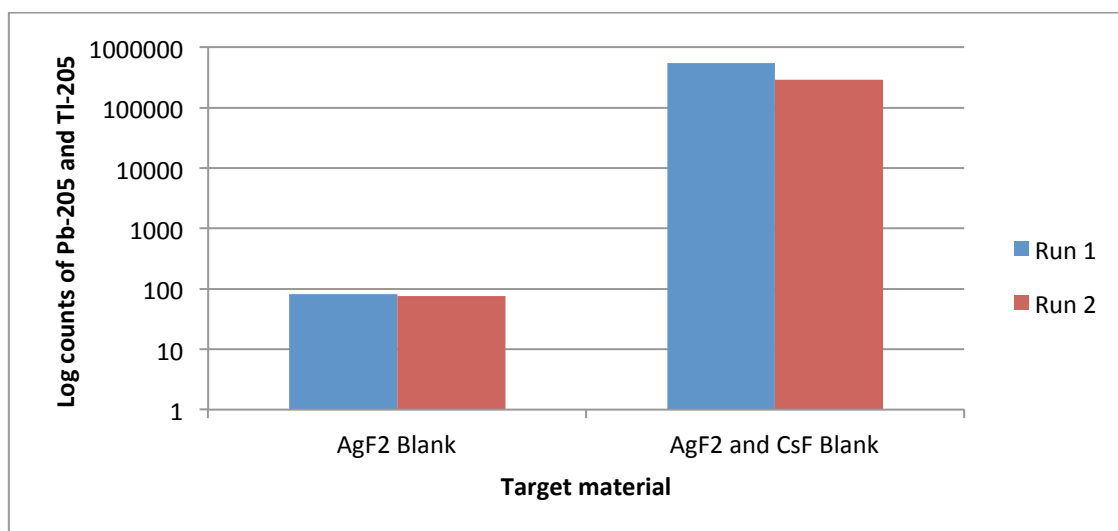


**Figure 9** Counts at mass-to-charge 205 for blanks of AgF<sub>2</sub> and blanks of AgF<sub>2</sub> and CsF. Note the log scale.

The <sup>205</sup>Tl inference could be swamped if larger amounts of <sup>205</sup>Pb are used; however, due to cost of <sup>205</sup>Pb this may not be feasible, unless more <sup>205</sup>Pb becomes available. In addition, the loss in ionization efficiency from packing targets without CsF, makes <sup>205</sup>Pb a poor spike when trying to maximize efficiency for quantification of <sup>210</sup>Pb by AMS.

<sup>208</sup>Pb is common, inexpensive and suffers from no interferences.<sup>[22, 24]</sup> <sup>208</sup>Pb may be used for measurements of <sup>210</sup>Pb but there is limit to how much <sup>208</sup>Pb can be added to targets without tailing or spill over into the <sup>210</sup>Pb channels of the energy spectrum this known as abundance sensitivity.<sup>[4]</sup> In an AMS measurement the abundance sensitivity depends on the resolution of the low energy and high energy magnetic analyzers at the IsoTrace AMS facility. The scatter tail from <sup>208</sup>Pb to measurements of <sup>210</sup>Pb was determined to be  $1.8 \times 10^{-6}$  for the low energy magnet and for the high energy magnet it was  $7.1 \times 10^{-7}$ . The combination of both scatter tails suggest an abundance sensitivity of  $^{210}\text{Pb}/^{208}\text{Pb} = 1.3 \times 10^{-12}$ , or  $^{210}\text{Pb}/\text{Pb} = 6.8 \times 10^{-13}$ . Therefore, targets spiked with <sup>208</sup>Pb were prepared with isotope ratios that were under this threshold. Since <sup>208</sup>Pb suffers from no isobaric or molecular interferences it is an ideal spike for <sup>210</sup>Pb measurements. However, in order to measure <sup>210</sup>Pb the interference from <sup>140</sup>Ce must be removed.

$^{210}\text{Pb}^{+3}$  suffers from an interference high concentrations of ( $^{70}\text{Zn}^{+1}$ )-( $^{140}\text{Ce}^{+2}$ ) when both ions enter the detector in coincidence. Therefore, a reduction in either  $^{70}\text{Zn}$  and/or  $^{140}\text{Ce}$  reduces the counts in the  $^{210}\text{Pb}^{+3}$  energy region of interest. In order to remove these interferences from targets, a column chemistry technique used in geochronology was adapted.<sup>[15,16,17]</sup> The technique was tested using the standard references material, CLV-1.<sup>[23]</sup> Samples were digested in aqua regia and then Ce was extracted with an Ag1x8 resin column. Using this process  $^{140}\text{Ce}$  counts were reduced by a factor of 1000, while Zn counts remained high, figure 10. The reduction in  $^{140}\text{Ce}$  decreased the probability of the formation ( $^{70}\text{Zn}^{+1}$ )-( $^{140}\text{Ce}^{+2}$ ) complex. Therefore, to determine  $^{210}\text{Pb}$  by AMS targets can be spiked with  $^{208}\text{Pb}$  and then Ce removed with an AG1x8 resin to avoid false counts in the  $^{210}\text{Pb}^{+3}$  channel. This technique was used in subsequent measurements.

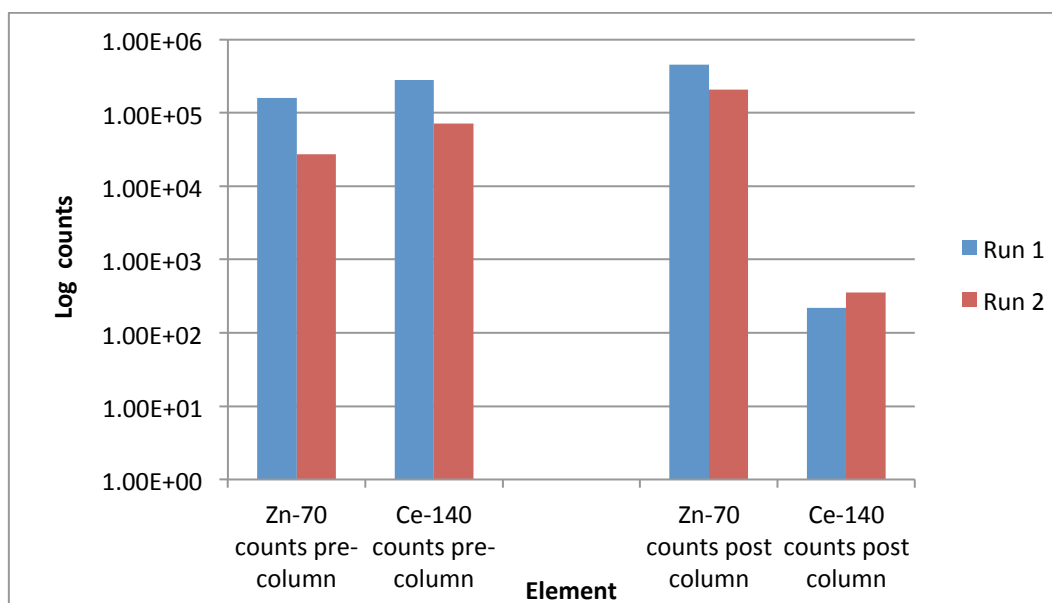


**Figure 10.** The counts of  $^{70}\text{Zn}^{+1}$  and  $^{140}\text{Ce}^{+2}$  at mass-to-charge  $^{210}/3$  pre- and post treatment with Ag1x8 column. Targets were composed of CLV-1 packed with  $\text{AgF}_2$  and  $\text{CsF}$  and each target was counted for 360sec.

Measurements of  $^{210}\text{Pb}$  by AMS were made by spiking the target with  $^{208}\text{Pb}$  and passing the sample through an Ag1x8 resin to remove  $^{140}\text{Ce}$  contamination. Known amounts of  $^{210}\text{Pb}$  were added to targets and measured by AMS in order to ensure accuracy of this AMS technique, table 6. The overall efficiency for  $^{210}\text{Pb}$  and  $^{208}\text{Pb}$ , were  $1.8 \times 10^{-10} \pm 8 \times 10^{-11}$ s and  $1.1 \times 10^{-9} \pm 9 \times 10^{-10}$ s<sup>-1</sup>, respectively

table 6. This difference in efficiencies is because  $^{210}\text{Pb}^{+3}$  ions were collected in the gas ionization chamber while  $^{208}\text{Pb}^{+3}$  ions were collected in a off-axis Faraday cup.

**Table 6** Measurements of targets spiked with known amounts of  $^{208}\text{Pb}$  and known activity of  $^{210}\text{Pb}$ . All targets were packed with equal parts by weight of  $\text{AgF}_2$  and  $\text{CsF}$ .

Target	Concentration of $^{208}\text{Pb}$ spike ( $\mu\text{g}$ )	Activity of $^{210}\text{Pb}$ (mBq)	$^{208}\text{Pb}$ collected (ng)	$^{210}\text{Pb}$ counts	$^{210}\text{Pb}$ activity based on isotope dilution (mBq)
1	113	857	0.42	$1.37 \times 10^3$	365
2	111	943	0.46	$1.62 \times 10^3$	383
3	108	730	0.12	236	217
4	114	760	0.37	112	341
5	108	730	0.05	123	255
6	112	100	0.09	46	54
7	108	100	0.12	36	32
8 <sup>a</sup>	111	66	0.16	23	17
9 <sup>a</sup>	110	66	0.59	12	2
10 (blank)	110	-	0.47	0	-
11 (blank)	111	-	0.49	4	-
12 (blank)	108	-	0.38	0	-
13 (blank)	107	-	0.39	1	-
14 (blank)	106	-	0.42	1	-
15 (blank)	108	-	0.37	1	-

The  $^{208}\text{Pb}^{+3}$  current was collected in a Faraday cup, because the number of  $^{208}\text{Pb}$  ions was so large that they would break the silica nitride window of the gas ionization chamber. The opening in the Faraday cup is such that almost all  $^{208}\text{Pb}^{+3}$  are collected, so little to no loss was expected. However, when the  $^{210}\text{Pb}^{+3}$  ions reach the gas ionization chamber they pass through a small silica nitride window (5mm x 5mm). This window is smaller than the  $^{210}\text{Pb}^{+3}$  beam spot size arriving at that window, thus some

$^{210}\text{Pb}^{+3}$  ions are lost. Previous work on the atomic beam of  $^{129}\text{I}^{+3}$  estimated that there was 20-30% loss of  $^{129}\text{I}^{+3}$  ions entering the gas ionization detector.<sup>[25]</sup> When the molecular ions  $^{210}\text{PbF}_3^-$  undergo a coulomb explosion in the tandem accelerator to generate  $^{210}\text{Pb}^{+3}$  ions, the ion beam may be more spread out than a  $^{129}\text{I}^{+3}$  ion beam. This leads to an additional loss of  $^{210}\text{Pb}$  atoms as some  $^{210}\text{Pb}$  atoms did not enter the small opening at the silica nitrate window. Furthermore,  $^{210}\text{Pb}^{+3}$  ions travel an extra ~15meters to reach the gas ionization chamber with losses expected along that flight path. The difference in efficiency may be corrected for by using a calibration curve or an efficiency measurement, figure 11.

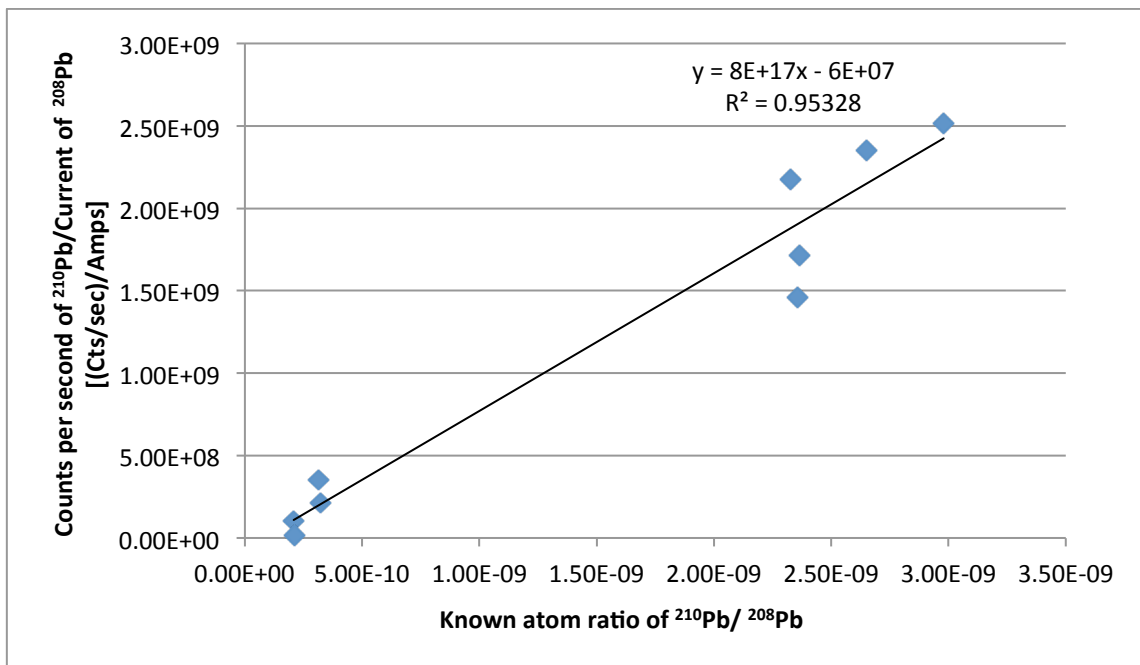


**Figure 11** Calibration curve for  $^{210}\text{Pb}$  counts with respect to  $^{208}\text{Pb}$  spike targets count timed ranged 1280-3000s

The correlation coefficient of 0.95 suggests that this type of calibration curve is a viable way to account for the differences in efficiencies of  $^{208}\text{Pb}$  and  $^{210}\text{Pb}$ . Although, a calibration curve is no additional preparation time is required as standards can be prepared along with unknown samples.

Blank samples were measured that contained no  $^{210}\text{Pb}$ . One to 4 counts were collected in the  $^{210}\text{Pb}$  spectrum over a period of  $1.6 \times 10^3$  seconds. The average blank is 1.16 counts with a standard

deviation of 1.47 in  $1.6 \times 10^3$  seconds using the calibration described previously. This blank corresponds to a detection limit for  $^{210}\text{Pb}$  of 4.4mBq in  $5.4 \times 10^3$ s. The detection limit was calculated as three times the standard deviation of the blank samples. The detection limit was controlled by the overall efficiency for  $^{210}\text{Pb}$ , table 7. At the newly established AMS at A.E. Lalonde facility a theoretical detection limit of  $\leq 0.11$ mBq is expected due to an improved ion source (a SO-110), and better transmission through the AMS system.

**Table 7** Detection limits for  $^{210}\text{Pb}$  at the IsoTrace Laboratory and A.E Lalonde Laboratory.

AMS Facility	Overall efficiency for $^{210}\text{Pb}$	Detection limit in $5.4 \times 10^3$ s
IsoTrace Laboratory	$1.8 \times 10^{-10} \pm 8 \times 10^{-11}$ s	4.4mBq
A.E Lalonde Laboratory	$7.2 \times 10^{-9} \pm 3.2 \times 10^{-9}$	$\leq 0.11$ mBq*

\*Assumes same background as IsoTrace facility. New system most likely is better at separating out interferences

## CONCLUSION

$^{210}\text{Pb}$  was measured by AMS.  $\text{PbF}_3^-$  was extracted from the ion source and  $\text{Pb}^{+3}$  was accelerated into the ionization detector. The measurement of isotopes of Pb were complicated by the presence of several molecular and isobaric interferences. The interferences of  $^{140}\text{Ce}$  was removed by using an Ag1x8 resin. The simplest method to quantify the amount of  $^{210}\text{Pb}$  in the sample was to spike with  $\mu\text{g}$  of  $^{208}\text{Pb}$ . Interferences of  $^{204}\text{Pb}$  were not removed easily and the use of  $^{205}\text{Pb}$  precludes the use of CsF, which reduces the production of  $\text{PbF}_3^-$  anions. Using  $^{208}\text{Pb}$  as spike our detection limit was 4.4mBq for  $^{210}\text{Pb}$ . The main limitation to better detection is the low efficiency for  $\text{Pb}^{+3}$  ions at the IsoTrace facility in Toronto, Canada. A theoretical detection limit of  $\leq 0.11$ mBq for  $^{210}\text{Pb}$  is expected at the A.E Lalonde AMS facility. Further investigation also is required into measurements using the  $\text{Pb}^{+1}$  and  $\text{Pb}^{+2}$  states since these are more abundant than the  $\text{Pb}^{+3}$  charge state used in this work.

## Acknowledgements

The Isotracer laboratory that was operated by the University of Ottawa at its original location in Toronto but has since relocated to the A.E.L. lab in Ottawa. A.E.L. laboratory acknowledges the support through Canada Innovation for Foundation and grants through NSERC. We also gratefully acknowledge the Jack Satterly Geochronology laboratory for supplying  $^{205}\text{Pb}$ .

## REFERENCES

- [1] F. Oldfield, P.G. Appleby. Empirical testing of  $^{210}\text{Pb}$ -dating models for lake sediments. *Lake Sed. Environ. Hist.* **1984**, 15, 93.
- [2] K.H. Rubin, I. Van der Zander, M.C. Smith, E.C. Bergmanis. Minimum speed limit for ocean ridge magmatism from  $^{210}\text{Pb}$ – $^{226}\text{Ra}$ – $^{230}\text{Th}$  disequilibria. *Nature*. **2005**437, 534.
- [3] L.A. Ladinskaya, Y.D. Parfenov, D.K. Popov, A.V. Fedorova.  $^{210}\text{Pb}$  and  $^{210}\text{Po}$  content in air, water, foodstuffs, and the human body. *Archives of Environ. Health: An International J.* **1973**, 27, 254.
- [4] D. Larivière, K.M. Reiber, R.D. Evans, R.J. Cornett. Determination of  $^{210}\text{Pb}$  at ultra-trace levels in water by ICP-MS. *Anal. Chim. Acta.* **2005**, 549, 188.
- [5] X. Hou, P. Roos. (2008). Critical comparison of radiometric and mass spectrometric methods for the determination of radionuclides in environmental, biological and nuclear waste samples. *Anal. Chim. Acta.* **2008**, 608, 105.
- [6] M.A. Amr, K.A. Al-Saad, A.I. Helal, Ultra-trace Measurements of  $^{210}\text{Pb}$  in natural occurring radioactive materials by ICP-MS. *Nucl. Instrum. Methods* **2010**, A615, 237.
- [7] Q.J. Chen, X.L. Hou, H. Dahlgard, S.P. Nielsen, A. Aarkrog. A rapid method for the separation of  $^{210}\text{Po}$  from  $^{210}\text{Pb}$  by TIOA extraction. *J. Radioanal. Nucl. Chem.* **2001**, 249, 587.
- [8] Y.Y. Ebaid, A.E.M. Khater. Determination of  $^{210}\text{Pb}$  in environmental samples. *J. Radioanal. Nucl. Chem.* **2006**, 270, 609.
- [9] Hermanson, M. H.  $^{210}\text{Pb}$  and  $^{137}\text{Cs}$  chronology of sediments from small, shallow Arctic lakes. *Geochimica et Cosmochimica Acta.* **1990**54, 1443.
- [10] G. Kirchner, H. Ehlers. Sediment geochronology in changing coastal environments: potentials and limitations of the  $^{137}\text{Cs}$  and  $^{210}\text{Pb}$  methods. *J. Coastal Res.* **1998**, 483.
- [11] X.-L. Zhao, A. E. Litherland, J. Eliades, W. E. Kieser, Q. Liu. Studies of anions from sputtering I: Survey of  $\text{MF}_n$ . *Nucl. Instrum. Methods* **2010**, B268, 807.
- [12] X.-L. Zhao, W. E. Kieser, X. Dai, N. D. Priest, S. Kramer-Tremblay, J. Eliades, A. E. Litherland. Preliminary studies of Pu measurement by AMS using  $\text{PuF}_4$ . *Nucl. Instrum. Methods* **2013**, B294, 356.
- [13] J.S. Vogel, K.W. Turteltaub, R. Finkel, D.E. Nelson. Accelerator mass spectrometry. *Anal. Chem.* **1995**, 67, 353A.
- [14] A. Sookdeo, J. Cornett, X.L. Zhao, W.E. Keiser. Production of Pb beams for  $^{205,210}\text{Pb}$  analysis by AMS. Submitted to *Nucl. Instrum. Methods*
- [15] G. Manhès, J.F. Minster, C.J. Allègre. Comparative uranium–thorium–lead and rubidium–strontium study of the Saint Severin amphibole; consequences for early solar system chronology Earth Planet. *Sci. Lett.* **1978**, 39, 14
- [16] C. Göpel, G. Manhès, C.J. Allègre U–Pb systematics in iron meteorites: uniformity of primordial lead. *Geochim. Cosmochim. Acta.* **1985**, 49, 1681.
- [17] C.R.J. Charles PhD Thesis, University of Toronto. **2013**
- [18] Parrish, R. R., & Krogh, T. E. Synthesis and purification of  $^{205}\text{Pb}$  for U Pb geochronology. *Chem. Geo. Isotope Geosci. Sec.* **1987**66, 103.

- [19] A.J. Bednar, V.F. Medina, D.S. Ulmer-Scholle, B.A. Frey, B.L. Johnson, W.N. Brostoff, S.L. Larson. Effects of organic matter on the distribution of uranium in soil and plant matrices. *Chemosphere*. **2007**70, 237
- [20] L. R. Kilius, N. Baba, M. A. Garwan, A.E. Litherland, M.J. Nadeau, J.C. Rucklidge, G.C. Wilson, X.-L. Zhao. (1990). AMS of heavy ions with small accelerators. *Nucl. Instrum. Methods*. **1990** B52, 357.
- [21] X.-L. Zhao, M.J. Nadeau, L.R. Kilius, A.E. Litherland. The first detection of naturally-occurring  $^{236}\text{U}$  with accelerator mass spectrometry. *Nucl. Instrum. Methods*. **1994**B92, 249.
- [22] W.U. Ault, R.G. Senechal, W.E. Erlebach. Isotopic composition as a natural tracer of lead in the environment. *Enviro. Sci.Tech*. **1970**, 4, 305.
- [23] Middleton, R. A review of ion sources for accelerator mass spectrometry. *Nucl. Instrum. Methods*. **1984** B5, 193.
- [24] E.T. Rasbury, W.J. Meyers, G.N. Hanson, R.H. Goldstein, A.H. Saller. Relationship of uranium to petrography of caliche paleosols with application to precisely dating the time of sedimentation. *J. of Sediment. Res.* **2000**70, 604.
- [25] L.R. Kilius, X.L. Zhao, A.E. Litherland, K.H. Purser. (1997). Molecular fragment problems in heavy element AMS. *Nucl. Instrum. Methods*. **1997** B123, 10.

## CHAPTER 4

### Conclusions

The aim of this thesis was to establish the methodology to measure  $^{210}\text{Pb}$  by Accelerator Mass Spectrometry (AMS). The second goal was to test the hypothesis that AMS can detect  $^{210}\text{Pb}$  below the established detection limits of radiometric and mass spectrometry techniques, the best of those being  $\alpha$  spectroscopy. The determination of  $^{210}\text{Pb}$  by AMS was done in two major studies 1) Studying Pb chemistry in a  $\text{Cs}^+$  sputter source used in AMS and 2) Evaluating  $^{204,205}$  &  $^{208}\text{Pb}$  spikes for the quantification of  $^{210}\text{Pb}$  by isotope dilution.

The production of Pb beams was investigated with a 834 SIMS-type  $\text{Cs}^+$  sputter source at the IsoTrace Laboratory and with a SO-110  $\text{Cs}^+$  sputter source at the A.E Lalonde AMS facility. By studying different molecular anions of Pb in the  $\text{Cs}^+$  sputter source I established the strongest Pb current and thus greatest ionization efficiency was achieved from the superhalogen  $\text{PbF}_3^-$ . The ratio of fluorinating,  $\text{AgF}_2$  and  $\text{CsF}$  agent packed into the Pb target does not affect the current of  $^{208}\text{PbF}_3^-$  as both are strong oxidizers. The current of  $^{208}\text{PbF}_3^-$  was increased by chemically mixing the targets of  $\text{AgF}_2$ ,  $\text{CsF}$  and  $\text{PbF}_2$  in concentrated HF rather than mechanically mixing them with a stir rod, and the homogeneity of target likely increased. When  $\mu\text{g}$  quantities of  $\text{PbF}_2$  are present in mg AMS targets the ion conductivity of the target is increased due to a phase change of  $\text{PbF}_2$  at higher temperatures. The phase change promotes interactions of  $\text{F}^-$  anions in AMS targets resulting in a larger production of  $\text{PbF}_3^-$ . Furthermore, in an SO-100  $\text{Cs}^+$  sputter source the average current of  $^{208}\text{PbF}_3^-$  is higher using a  $\text{Cs}^+$  flux that generated  $5\mu\text{A}$  of  $^{12}\text{C}^-$  current than using a  $\text{Cs}^+$  flux that generated  $50\mu\text{A}$  of  $^{12}\text{C}^-$  current. This phase of my work maximized the overall efficiency of  $\text{PbF}_3^-$  production,  $1.8 \times 10^{-10} \pm 8 \times 10^{-11} \text{s}^-$ , which was a key first step in the measurement by AMS. Isotope dilution was tested to quantify  $^{210}\text{Pb}$  and the next stage of my work evaluated the use of  $^{204,205}$  &  $^{208}\text{Pb}$  spikes.

$^{204,205}$  &  $^{208}\text{Pb}$  spikes were evaluated in a +3 charge state for isotope dilution measurements of  $^{210}\text{Pb}$ .  $^{204}\text{Pb}^{+3}$  was collected in Faraday cup and suffered from the molecular interference from  $^{68}\text{Zn}_3^{+3}$ ,

which could not be easily removed without sacrificing overall efficiency for Pb thus negatively impacting the detection limit.  $^{205}\text{Pb}^{+3}$  suffered primarily from  $^{205}\text{Tl}^{+3}$ , which could be removed by eliminating CsF from the target. This would however sacrifice Pb ionization efficiency and this would negatively affect the detection limit. In addition, both  $^{204,205}\text{Pb}$  are expensive isotopes and to spike with  $\mu\text{g}$  quantities for reasons mentioned previously, would be financial infeasible. There is a limit to the amount of  $^{208}\text{Pb}$  that can be present in the AMS targets since the abundance sensitivity of  $^{210}\text{Pb}/^{208}\text{Pb}=1.3\times 10^{-12}$  could limit the detection limit for  $^{210}\text{Pb}$ . Further,  $^{208}\text{Pb}^{+3}$  ions are collected in an off-axis Faraday cup, while  $^{210}\text{Pb}^{+3}$  is collected in gas ionization chamber. There is a difference in collection efficiency of the detectors so a calibration curve is required when using  $^{208}\text{Pb}$  for isotope dilution of  $^{210}\text{Pb}$ . The quantification of  $^{210}\text{Pb}$  with  $^{208}\text{Pb}$  as a spike yields a detection limit of 4.4mBq at the IsoTrace facility and a theoretical detection limit of  $\leq 0.1$  mBq is expected at the A.E Lalonde AMS facility. The expected detection limit at the A.E Lalonde AMS facility is on par with  $\alpha$ -spectroscopy but AMS samples can be counted in less than 1 hour whereas alpha spectrometry samples must be counted for about 1 day.

In summary, this work has demonstrated that  $^{210}\text{Pb}$  can be measured efficiently by AMS. To improve on the detection limit of  $^{210}\text{Pb}$  by AMS, in order to measure  $^{210}\text{Pb}$  in people exposed to typical levels of radon present in indoor air, I recommend future studies to test measurements by AMS of Pb ions in charge states of  $\text{Pb}^{+1}$  and  $\text{Pb}^{+2}$ . These charge states are much more abundant than the  $\text{Pb}^{+3}$  charge state studied in this work. In addition, further investigation the formation of  $\text{PbF}_3^-$  in a SO-110  $\text{Cs}^+$  sputter source is required to improve the beam current and to reduce the detection limit of  $^{210}\text{Pb}$  by AMS.